Theoretical Study of the Cp₂Zr-Catalyzed Hydrosilylation of Ethylene. Reaction Mechanism Including New σ-Bond Activation

Shigeyoshi Sakaki,*,† Tatsunori Takayama,‡ Michinori Sumimoto,† and Manabu Sugimoto‡

Contribution from the Department of Molecular Engineering, Graduate School of Engineering, Kyoto University, Nishikyou-ku, Kyoto 615-8510, Japan, and Department of Applied Chemistry and Biochemistry, Graduate School of Science and Technology, Kumamoto University, Kumamoto 860-8555, Japan

Received July 16, 2003; Revised Manuscript Received December 22, 2003; E-mail: sakaki@moleng.kyoto-u.ac.jp

Abstract: The Cp₂Zr-catalyzed hydrosilylation of ethylene was theoretically investigated with DFT and MP2−MP4(SDQ) methods, to clarify the reaction mechanism and the characteristic features of this reaction. Although ethylene insertion into the Zr−SiH₃ bond of Cp₂Zr(H)(SiH₃) needs a very large activation barrier of 41.0 (42.3) kcal/mol, ethylene is easily inserted into the Zr−H bond with a very small activation barrier of 2.1 (2.8) kcal/mol, where the activation barrier and the energy of reaction calculated with the DFT-(B3LYP) method are given and in parentheses are those values which have been corrected for the zero-point energy, hereafter. Not only this ethylene insertion reaction but also the coupling reaction between Cp₂Zr(C₂H₄) and SiH₄ easily takes place to afford Cp₂Zr(H)(CH₂CH₂SiH₃) and Cp₂Zr(CH₂CH₃)(SiH₃) with activation barriers of 0.3 (0.7) and 5.0 (5.4) kcal/mol, respectively. This coupling reaction involves a new type of Si−H σ-bond activation which is similar to metathesis. The important interaction in the coupling reaction is the bonding overlap between the d$_\pi$-π* bonding orbital of Cp₂Zr(C₂H₄) and the Si−H σ* orbital. The final step is neither direct C−H nor Si−C reductive elimination, because both reductive eliminations occur with a very large activation barrier and significantly large endothermicity. This is because the d orbital of Cp₂Zr is at a high energy. On the other hand, ethylene-assisted C−H reductive elimination easily occurs with a small activation barrier, 5.0 (7.5) kcal/mol, and considerably large exothermicity, −10.6 (−7.1) kcal/mol. Also, ethylene-assisted Si−C reductive elimination and metatheses of Cp₂Zr(H)(CH₂CH₂SiH₃) and Cp₂Zr(CH₂CH₃)(SiH₃) with SiH₄ take place with moderate activation barriers, 26.5 (30.7), 18.4 (20.5), and 28.3 (31.5) kcal/mol, respectively. From these results, it is clearly concluded that the most favorable catalytic cycle of the Cp₂Zr-catalyzed hydrosilylation of ethylene consists of the coupling reaction of Cp₂Zr(C₂H₄) with SiH₄ followed by the ethylene-assisted C−H reductive elimination.

Introduction

The transition-metal-catalyzed hydrosilylation of alkene is one of the important synthetic reactions of organic silicon compounds.[1] This reaction is of considerable interest from both points of view of organometallic chemistry and theoretical chemistry because of several reasons: one of them is that the catalytic cycle involves many interesting elementary steps including σ-bond activation and alkene insertion into the M−H or M−SiR₃ bond, and the other is that the reaction mechanism is flexible and depends on the kinds of transition-metal elements.[1] For instance, the Chalk−Harrod mechanism was proposed for the platinum-catalyzed hydrosilylation of alkene,[1,2]

which consists of the Si−H σ-bond activation of silane by a transition metal complex, alkene insertion into the M−H bond, and Si−C reductive elimination, as shown in Scheme 1. Later, the modified Chalk−Harrod mechanism was proposed for the rhodium-catalyzed hydrosilylation of alkene, which consists of the Si−H σ-bond activation of silane by a transition metal complex like that in the Chalk−Harrod mechanism, alkene insertion into the M−SiR₃ bond, and C−H reductive elimination, as shown in Scheme 1.[1,3−10] Evidence of this mechanism is that vinylsilane is produced as a byproduct in the rhodium-

† Kyoto University.
‡ Kumamoto University.
(1) (a) Tilley, T. D. In *The Chemistry of Organic Silicon Compounds*; Patai, S., Rappoport, Z., Eds.; John Wiley & Sons Ltd.: New York, 1989; p 1415. (b) Ojima, I. In *The Chemistry of Organic Silicon Compounds*; Patai, S., Rappoport, Z., Eds.; John Wiley & Sons Ltd.: New York, 1989; p 1479. (c) Collman, J. P.; Hegedus, L. S.; Norton, J. R.; Finke, R. G. *Principles and Applications of Organotransition Metal Chemistry*; University Science Books: Mill Valley, CA, 1987; p 564.
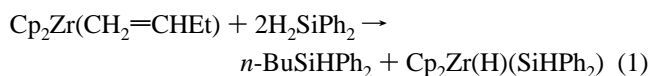
(2) Chalk, A. J.; Harrod, J. F. *J. Am. Chem. Soc.* **1965**, *87*, 16.
(3) (a) Schroeder, M. A.; Wrighton, M. S. *J. Organomet. Chem.* **1977**, *128*, 345. (b) Reichel, C. L.; Wrighton, M. S. *Inorg. Chem.* **1980**, *19*, 3835. (c) Randolph, C. L.; Wrighton, M. S. *J. Am. Chem. Soc.* **1986**, *108*, 3366. (d) Seitz, F.; Wrighton, M. S. *Angew. Chem., Int. Ed. Engl.* **1988**, *27*, 289.
(4) (a) Milan, A.; Towns, E.; Maitlis, P. M. *J. Chem. Soc., Chem. Commun.* **1981**, 673. (b) Milan, A.; Fernandez, M.-J.; Bentz, P.; Maitlis, P. M. *J. Mol. Catal.* **1984**, *26*, 89.
(5) (a) Onopchenko, A.; Sabourin, E. T.; Beach, D. L. *J. Org. Chem.* **1983**, *48*, 5101. (b) Onopchenko, A.; Sabourin, E. T.; Beach, D. L. *J. Org. Chem.* **1984**, *49*, 3389. (c) Onopchenko, A.; Sabourin, E. T.; Beach, D. L. *J. Org. Chem.* **1987**, *52*, 4118.

Scheme 1
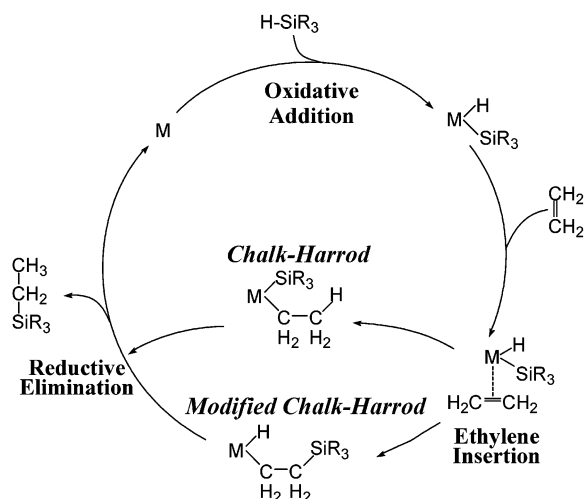
catalyzed hydrosilylation of alkene; because vinylsilane is formed from $M(H)(CH_2CH(R)SiR_3)$ (or $M(H)(CH(R)CH_2SiR_3)$) through β-H abstraction, formation of vinylsilane means that alkene is inserted into the $M-SiR_3$ bond.[3–7,10] However, we should remember the possibility that formation of vinylsilane does not necessarily mean there is evidence of the modified Chalk−Harrod mechanism, because it can be produced through the C−H σ-bond activation of alkene followed by the reductive elimination between vinyl and silyl groups.[11] Other evidence is the spectroscopic detection of $Cp^*Co[P(OMe)_3][CH(Bu)CH-(SiEt_3)-\mu-H]^+$ in the cobalt-catalyzed hydrosilylation of alkene.[12] We theoretically investigated both the platinum-catalyzed hydrosilylation of ethylene[13] and the rhodium-catalyzed hydrosilylation of ethylene[14] and clarified the reasons that the platinum-catalyzed and the rhodium-catalyzed hydrosilylations take place through Chalk−Harrod and modified Chalk−Harrod mechanisms, respectively.[13,14]

However, the third mechanism was experimentally suggested by Takahashi, Negishi, and their collaborators,[15] in which the product was produced through the reaction of $Cp_2Zr(alkene)$ and silane (eq 1). Shortly thereafter, the catalytic cycle including the metathesis-like coupling reaction between $Cp_2Zr(alkene)$ and silane was proposed by Corey and his collaborator,[16] as shown

(6) (a) Ojima, I.; Yatabe, M.; Fuchikami, T. *J. Organomet. Chem.* **1984**, *260*, 335. (b) Ojima, I.; Clos, N.; Donovan, R. J.; Ingallina, P. *Organometallics* **1990**, *9*, 3127.
(7) Oro, L. A.; Fernandez, M. J.; Esteruelas, M. A.; Jimenez, M. S. *J. Mol. Catal.* **1986**, *37*, 151.
(8) Ruiz, J.; Bentz, P. O.; Mann, B. E.; Spencer, C. M.; Taylor, B. F.; Maitlis, P. M. *J. Chem. Soc., Dalton Trans.* **1987**, 2709.
(9) Bergens, S. H.; Noheda, P.; Whelan, J.; Bosnich, B. *J. Am. Chem. Soc.* **1992**, *114*, 2128.
(10) Duckett, S. B.; Peruz, R. N. *Organometallics* **1992**, *11*, 90.
(11) Vinylsilane is produced from alkenes through the C−H σ-bond activation of alkenes followed by reductive elimination between vinyl and silyl groups.[11b] This means that the formation of vinylsilane does not necessarily provide evidence of the modified Chalk−Harrod mechanism. (b) Ruiz, J.; Bentz, P. O.; Mann, B. E.; Spencer, C. M.; Taylor, B. F.; Maitlis, P. M. *J. Chem. Soc., Dalton Trans.* **1987**, 2709.
(12) Brookhart, M.; Grant, B. E. *J. Am. Chem. Soc.* **1993**, *115*, 2151.
(13) (a) Sakaki, S.; Ogawa, M.; Musashi, Y.; Arai, T. *J. Am. Chem. Soc.* **1994**, *116*, 7258. (b) Sakaki, S.; Mizoe, N.; Sugimoto, M. *Organometallics* **1998**, *17*, 2510. (c) Sakaki, S.; Mizoe, N.; Musashi, Y.; Sugimoto, M. *J. Mol. Struct. (THEOCHEM)* **1999**, *461–462*, 533. (d) Sakaki, S.; Mizoe, N.; Sugimoto, M.; Musashi, Y. *Coord. Chem. Rev.* **1999**, *190–192*, 933.
(14) Sakaki, S.; Sumimoto, M.; Fukuhara, M.; Sugimoto, M.; Fujimoto, H.; Matsuzaki, S. *Organometallics* **2002**, *21*, 3788.
(15) Takahashi, T.; Hasegawa, M.; Suzuki, N.; Saburi, M.; Rousset, C. J.; Fanwick, P. E.; Negishi, E.-I. *J. Am. Chem. Soc.* **1991**, *113*, 8564.
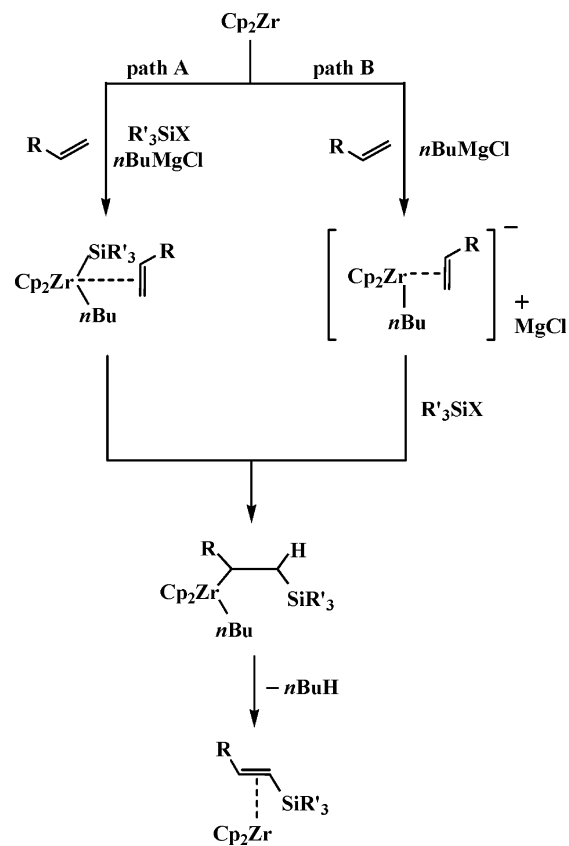(16) Corey, J. Y.; Zhu, X.-H. *Organometallics* **1992**, *11*, 672.

$$Cp_2Zr(CH_2=CHEt) + 2H_2SiPh_2 \rightarrow$$
$$n\text{-BuSiHPh}_2 + Cp_2Zr(H)(SiHPh_2) \quad (1)$$

in Scheme 2. Waymouth and his collaborator[17] also proposed a similar reaction mechanism, as shown in Scheme 3. In these reaction mechanisms, neither the alkene insertion into the Zr−H bond nor the alkene insertion into the Zr−SiR₃ bond is involved, but the coupling reaction between $Cp_2Zr(alkene)$ and silane is involved. Kambe and his collaborators catalytically synthesized vinylsilane from alkene and various silane, $X-SiPh_3$ (X = Cl, SPh, SePh, or TePh), with Cp_2ZrCl_2.[18] They suggested that vinylsilane was produced through not only alkene insertion into the Zr−SiR₃ bond but also the coupling reaction between Cp_2-$Zr(alkene)$ and silane, as shown in Scheme 4. Recently, Takahashi and his collaborators reported the reaction of Cp_2-$Zr(alkene)$ with chlorosilane and its Ge and Sn analogues, Cl−EPh_3 (E = Si, Ge, or Sn).[19] In their work, they proposed the coupling reaction between $Cp_2Zr(alkene)$ and H−SiR₃, as shown in Scheme 5. All of these reports suggest that the Cp_2Zr-catalyzed hydrosilylation of olefin proceeds through a new mechanism including the coupling reaction between Cp_2Zr-(alkene) and silane. However, there is no direct evidence of this coupling reaction, and it is ambiguous why this reaction can take place in the Cp_2Zr-catalyzed hydrosilylation of alkene.

On the other hand, insertion of ethylene into the Zr−silyl and Hf−silyl bonds was experimentally reported, while it occurred very slowly.[20] This report suggests that the zirconium-catalyzed hydrosilylation of alkene proceeds through the modified Chalk−Harrod mechanism. In the hydrosilylation of alkene catalyzed by organolanthanide and organoyttrium complexes which are similar to the organozirconium complexes, however, the Chalk−Harrod mechanism was proposed as a plausible mechanism, except that the product release step was not usual Si−C reductive elimination but σ-bond metathesis.[21–23] Above-mentioned reports indicate that there is considerable confusion in the discussion of the reaction mechanism of the zirconium-catalyzed hydrosilylation of alkene. Thus, a detailed investigation is necessary to clarify the catalysis of zirconium complexes. In this work, we theoretically investigated the Cp_2Zr-catalyzed hydrosilylation of alkene with the DFT and MP2−MP4(SDQ) methods. Our purposes are to elucidate the reaction mechanism and to clarify the reasons that the reaction mechanism of the Cp_2Zr-catalyzed hydrosilylation and the mechanisms of others such as Pt- and Rh-catalyzed hydrosilylations are different. Our emphasis of the efforts here is to present theoretically a very complicated new reaction mechanism which involves a new type of Si−H σ-bond activation reaction between $Cp_2Zr(alkene)$ and silane, to elucidate the key interaction that plays a crucial role in the coupling reaction, and to clarify the reason that the Cp_2-Zr-catalyzed hydrosilylation of alkene takes place through a very complicated reaction mechanism.

(17) Kesti, M. R.; Waymouth, R. M. *Organometallics* **1992**, *11*, 1095.
(18) Terao, J.; Torii, K.; Saito, K.; Kambe, N.; Baba, A.; Sonoda, N. *Angew. Chem., Int. Ed.* **1998**, *37*, 2653.
(19) Ura, Y.; Hara, R.; Takahashi, T. *Chem. Lett.* **1998**, 195.
(20) Arnold, J.; Engeler, M. P.; Elsner, F. H.; Heyn, R. H.; Tilley, T. D. *Organometallics* **1989**, *8*, 2284.
(21) Fu, P.-F.; Brand, L.; Li, Y.; Marks, T. J. *J. Am. Chem. Soc.* **1995**, *117*, 7157.
(22) Molander, G. A.; Nichols, P. J.; Noll, B. C. *J. Org. Chem.* **1998**, *63*, 2292.
(23) Dask, A. K.; Wang, J. Q.; Eisen, M. S. *Organometallics* **1999**, *18*, 4724.

Scheme 2 [a]
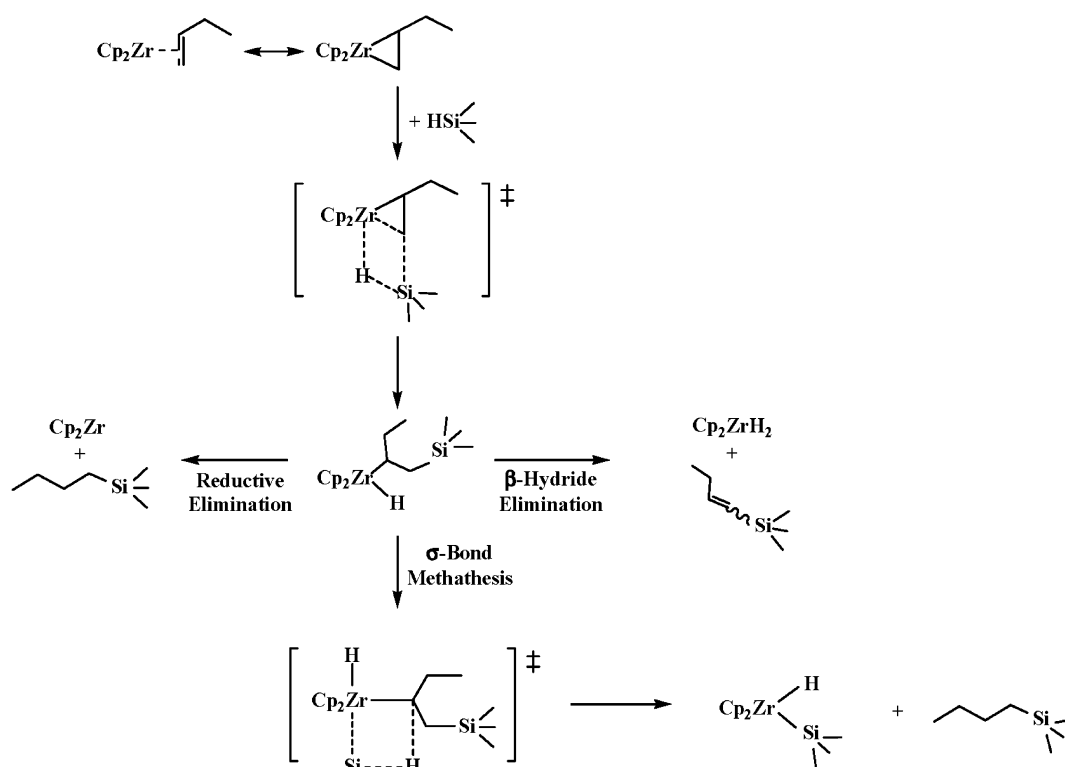
[a] Reference 16.

Scheme 3 [a]

[a] Reference 17.

Scheme 4 [a]
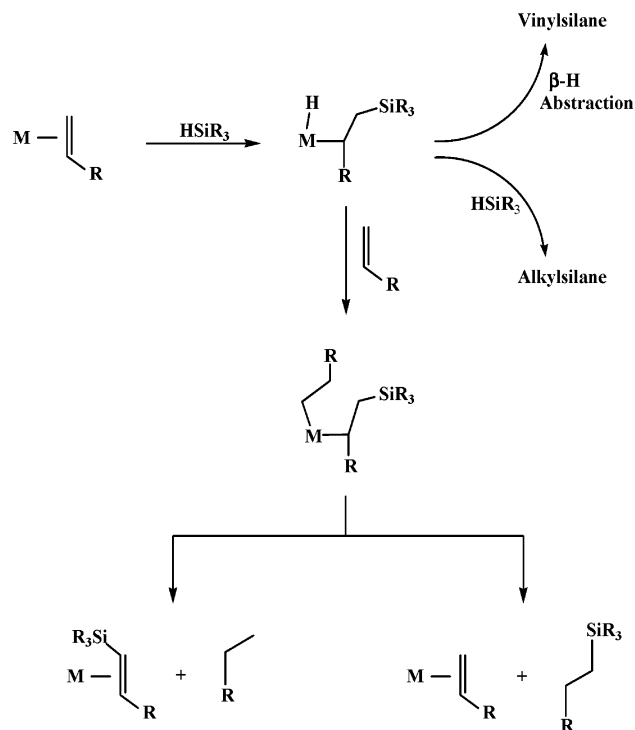
[a] Reference 18.

Computations and Models Adopted

Geometries were optimized with the DFT method, where the B3LYP functional was used.[24,25] Transition states were ascertained by perform-

ing a frequency calculation and examining what geometry changes are going to occur in the imaginary frequency. We present Supporting Information Figures S-1−S-8 to show the value of the imaginary

(24) (a) Becke, A. D. *Phys. Rev. A* **1988**, *38*, 3098. (b) Becke, A. D. *J. Chem. Phys.* **1983**, *98*, 5648.
(25) Lee, C.; Yang, W.; Parr, R. G. *Phys. Rev. B* **1988**, *37*, 785.

Scheme 5 [a]
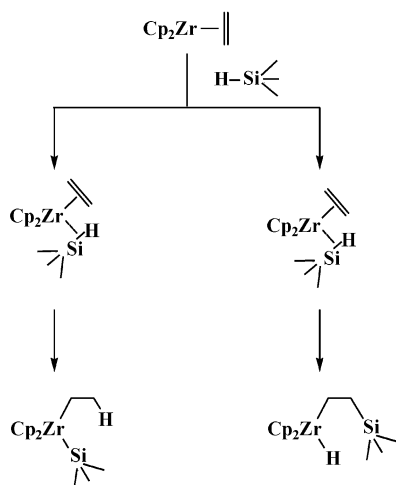
[a] Reference 19.

frequency and the geometry changes that are going to occur in the imaginary frequency.

Two kinds of basis set systems were used here. The smaller system (BS-I) was employed in geometry optimization. In this BS-I, core electrons (up to 3d) of Zr were replaced with effective core potentials (ECPs) proposed by Hay and Wadt, and its valence electrons were represented with a (311/311/111) set.[26] Core electrons of Si (up to 2p) were also replaced with ECPs, and its valence electrons were represented with a (21/21/1) set,[27] where a d-polarization function was added.[28] For C and H atoms, usual 6-31G basis sets[29] were used, where a d-polarization function was added to the C atom of ethylene and a p-polarization function was added to the hydride ligand and the H atom of SiH₄ that converts into the hydride ligand.[30] The better basis set system (BS-II) was employed in the evaluation of energy and population changes. In BS-II, a (541/541/211/1) set[26,31,32] was used for Zr with the same ECPs as those of BS-I. For Si, the Huzinage–Dunning (531111/521/1) set was employed[33] with a d-polarization function of which the exponent was taken from the works of the Schaefer group.[34] For C and H, 6-31G(d,p) sets were used,[29,30] where the d- and p-polarization functions were excluded from the Cp ligand.

We evaluated free energy changes at 298 K, in two ways. In one way, translation, rotation, and vibration movements were taken into consideration in the estimation of the thermal energy and free energy, where all substrates were treated as ideal gas. The DFT/BS-I method was adopted to calculate vibration frequencies without a scaling factor. In the other way, vibration movements were considered in the estimation of the thermal energy and free energy, but translation and rotation movements were not taken into consideration, because this hydrosilylation was carried out in solution in which the translation and rotation movements are highly suppressed. In the former method, entropy significantly decreases upon formation of adduct from two molecules, as expected. In the latter method, on the other hand, formation of adduct

induces a very small entropy change, as will be discussed below. The former method apparently overestimates the entropy effects and the thermal energy of the solution reaction, because translation and rotation movements are highly suppressed in solution. On the other hand, the latter method underestimates the entropy effects and the thermal energy, because translation and rotation movements are not completely suppressed in solution.[35] The true value would be intermediate between the value by the former method and that by the latter one, and more or less close to the free energy change estimated by the latter method, when the reaction is carried out in solution. Because this ambiguity remains in the estimation of the entropy and thermal energy, we will discuss each elementary step based on the usual total energy changes with and without zero-point energy correction. We will then discuss the energy changes along the entire catalytic cycle based on both the usual total energy change and the free energy change at 298 K. Of course, the free energy change does not differ so much from the total energy change in the elementary steps that involve neither the formation of adduct nor the release of product. Also, the free energy change that is evaluated by considering only vibration movements does not differ so much from the total energy change. The significant difference between the free energy change and the total energy change is observed in the elementary process that involves either the formation of adduct or the release of product, when translation, rotation, and vibration movements are considered in the estimation of free energy.

The Gaussian 98 program package was used for all of these calculations.[36] Population analysis was carried out with the method proposed by Weinhold et al.[37] Contour maps were drawn with the Molden program package.[38]

We carried out theoretical calculations with a real Cp₂Zr species, while we adopted SiH₄ and ethylene as models of silane and alkene, respectively, to save CPU time. In this work, we investigated the usual ethylene insertion into the Zr–H and Zr–SiH₃ bonds, because these reactions have been reported experimentally[20] and theoretically.[39] Also, we investigated the coupling reactions between Cp₂Zr(C₂H₄) and SiH₄ leading to Cp₂Zr(H)(CH₂CH₂SiH₃) and Cp₂Zr(SiH₃)(C₂H₅). A total of four reaction courses were examined. The final step is either the C–H reductive elimination of Cp₂Zr(H)(CH₂CH₂SiH₃) or the Si–C reductive elimination of Cp₂Zr(SiH₃)(C₂H₅), in general. We investigated both reductive eliminations because the ethylene insertion into the Zr–H bond of Cp₂Zr(H)(SiH₃) yields Cp₂Zr(SiH₃)(C₂H₅) and the coupling reaction between Cp₂Zr(C₂H₄) and SiH₄ yields Cp₂Zr(H)(CH₂CH₂SiH₃) and Cp₂Zr(SiH₃)(C₂H₅), as will be discussed below. In addition, we

(26) Hay, P. J.; Wadt, W. R. *J. Chem. Phys.* **1985**, *82*, 299.
(27) Wadt, W. R.; Hay, P. J. *J. Chem. Phys.* **1985**, *82*, 284.
(28) Höllwarth, A.; Böhme, M.; Dapprich, S.; Ehlers, A. W.; Gobbi, A.; Jonas, V.; Köhler, K. F.; Stegmann, R.; Veldkamp, A.; Frenking, G. *Chem. Phys. Lett.* **1993**, *208*, 237.
(29) Ditchfiled, P.; Hehre, W. J.; Pople, J. A. *J. Chem. Phys.* **1971**, *54*, 724.
(30) Hariharan, P. C.; Pople, J. A. *Mol. Phys.* **1974**, *27*, 209.
(31) Couty, M.; Hall, M. B. *J. Comput. Chem.* **1996**, *17*, 1359.
(32) Ehlers, A. W.; Böhme, M.; Dapprich, S.; Gobbi, A.; Höllwarth, A.; Jonas, V.; Köhler, K. F.; Stegmann, R.; Veldkamp, A.; Frenking, G. *Chem. Phys. Lett.* **1993**, *208*, 111.
(33) Dunning, T. H.; Hay, P. J. In *Methods of Electronic Structure Theory*; Schaefer, H. F., Ed.; Plenum: New York, 1977; p 1.
(34) The exponent (ζ = 0.50) of the 3d-polarization function of Si was taken from the many works of the Schaefer group. See, for instance: Brinkmann, N. R.; Tschumper, G. S.; Schaefer, H. F. *J. Chem. Phys.* **1999**, *110*, 6240 and references therein.

(35) In solution, translation and rotation movements are not completely free but are highly suppressed. This means that the thermal energy and the entropy deviate very much from the true values if we treat substrates as ideal gas. However, when we estimate the thermal energy and the entropy by considering only vibration movements, the values are underestimated, because translation and rotation movements are not completely suppressed but somewhat contribute to the thermal energy and the entropy in solution; for instance, the translation movement considerably occurs as shown by the rapid diffusion rate, and the rotation movement somewhat occurs in nonpolar solvent. Also, the solvation structure changes upon formation of the precursor complex, which contributes to the entropy effect. Unfortunately, we do not know how to estimate partition functions of translation and rotation movements in solution. One of the reasonable ways is to estimate thermal energy and entropy with and without translation and rotation movements and to compare free energy changes evaluated by two methods, as described in the text.
(36) Frisch, M. J.; Trucks, G. W.; Schlegel, H. B.; Scuseria, G. E.; Robb, M. A.; Cheeseman, J. R.; Zakrzewski, V. G.; Montgomery, J. A.; Stratmann, R. E.; Burant, J. C.; Dapprich, S.; Millam, J. M.; Daniels, A. D.; Kudin, K. N.; Strain, M. C.; Farkas, O.; Tomasi, J.; Barone, V.; Cossi, M.; Cammi, R.; Mennucci, B.; Pomelli, C.; Adamo, C.; Cliford, S.; Ochterski, J.; Petersson, G. A.; Ayala, P. Y.; Cui, Q.; Morokuma, K.; Malick, D. K.; Rabuck, A. D.; Raghavachari, K.; Foresman, J. B.; Cioslowski, J.; Ortiz, J. V.; Stefanov, B. B.; Liu, G.; Liashenko, A.; Piskorz, P.; Komaromi, I.; Gomperts, R.; Martin, R. L.; Fox, D. J.; Keith, T.; Al-Laham, M. A.; Peng, C. Y.; Nanayakkara, A.; Gonzalez, C.; Challacombe, M.; Gill, P. M. W.; Johnson, B. G.; Chen, W.; Wong, M. W.; Andres, J. L.; Head-Gordon, M.; Replogle, E. S.; Pople, J. A. *Gaussian 98*; Gaussian, Inc.: Pittsburgh, PA, 1998.
(37) Reed, A. E.; Curtis, L. A.; Weinhold, F. *Chem. Rev.* **1988**, *88*, 849 and references therein.
(38) Schaftenaar, G.; Noordik, J. H. *J. Comput.-Aided Mol. Des.* **2000**, *14*, 123.
(39) Endo, J.; Koga, N.; Morokuma, K. *Organometallics* **1993**, *12*, 2777.
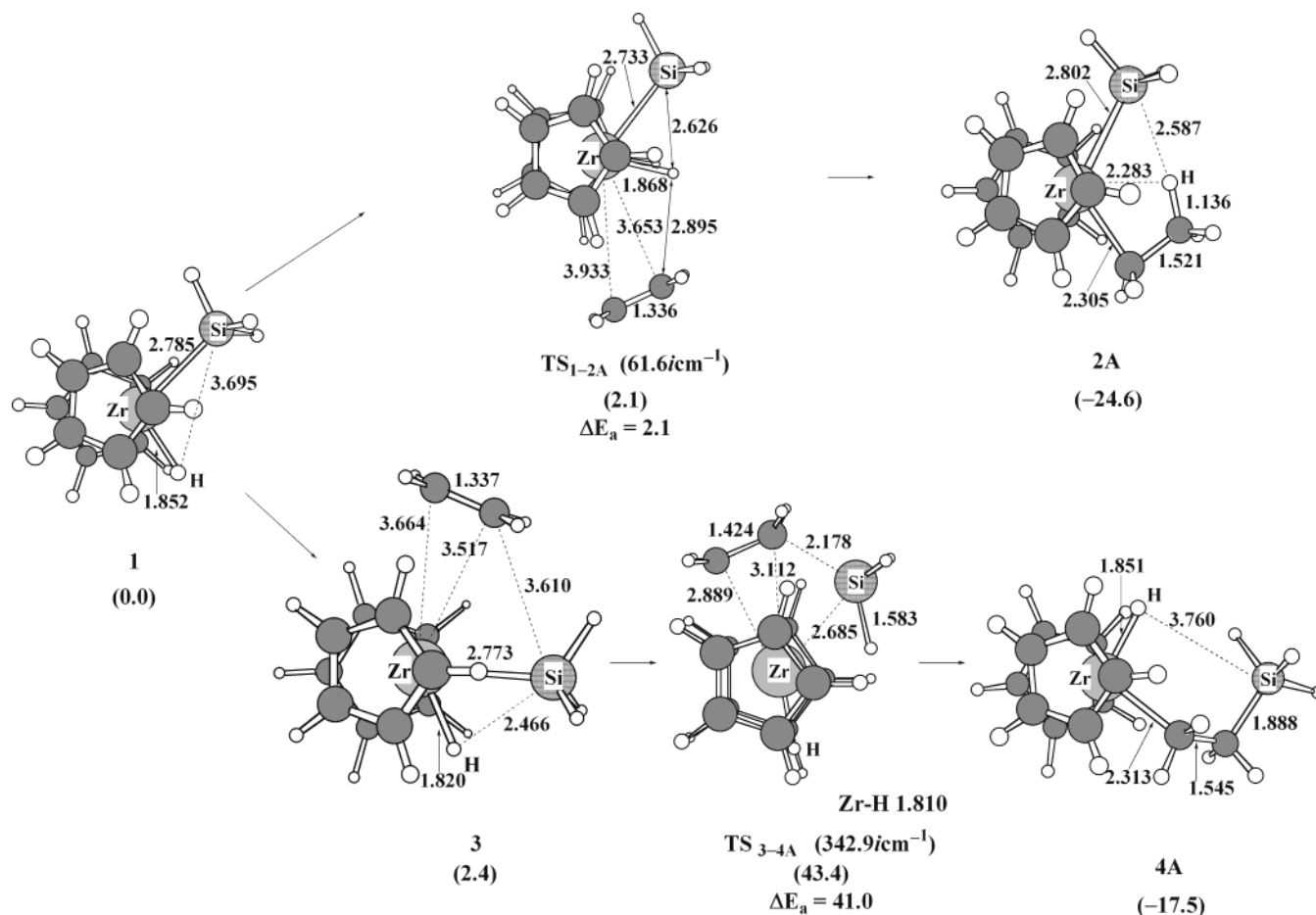
Figure 1. Geometry changes in the ethylene insertion into the Zr−H and Zr−SiH₃ bonds of Cp₂Zr(H)(SiH₃) **1**. Bond lengths are in angstroms. In parentheses are the relative energies (kcal/mol) to **1**, where the DFT(B3LYP)/BS-II method was employed.

investigated ethylene-assisted C−H and Si−C reductive eliminations and metatheses of Cp₂Zr(H)(CH₂CH₂SiH₃) and Cp₂Zr(SiH₃)(C₂H₅) with SiH₄, because direct C−H and Si−C reductive eliminations are difficult, as will be discussed below.

Results and Discussion

Reaction between Cp₂Zr(H)(SiH₃) and Ethylene. Because our present DFT calculations showed that the Si−H σ bond of SiH₄ easily underwent the oxidative addition to Cp₂Zr with no barrier, we omitted the discussion of the Si−H oxidative addition to the Cp₂Zr species. Here, we start to investigate the reaction of ethylene with Cp₂Zr(H)(SiH₃), **1**. As shown in Figure 1, ethylene approaches the Zr center through transition state **TS₁₋₂ₐ**, to afford an insertion product, Cp₂Zr(SiH₃)(C₂H₅), **2A**. The geometry of **TS₁₋₂ₐ** does not seem to correspond to ethylene insertion into the Zr−H bond, because the Zr−C and C−H distances are very long. Actually, geometry changes in the imaginary frequency correspond to the approach of ethylene to the Zr center and distortion of Cp₂Zr(H)(SiH₃), as shown in Supporting Information Figure S-1. Thus, this is the transition state for ethylene approach to the Zr center. However, an ethylene complex, Cp₂Zr(H)(SiH₃)(C₂H₄), could not be optimized, and the geometry optimization of this ethylene complex led to the insertion product, Cp₂Zr(SiH₃)(C₂H₅), **2A**; in other words, the ethylene insertion into the Zr−H bond proceeds with no barrier after this transition state. A similar result has been reported in the previous theoretical study of hydrozirconation,[39]

in which MP2 calculations showed that ethylene was easily inserted into the Zr−H bond with a small activation barrier of 3.8 kcal/mol.[39]

On the other hand, the other structure of the ethylene complex, Cp₂Zr(H)(SiH₃)(C₂H₄), **3**, could be optimized, in which ethylene took a position near the SiH₃ group, as shown in Figure 1. Although a transition state would exist between the reactant and **3** like **TS₁₋₂ₐ**, we omitted its optimization, because the ethylene insertion into the Zr−SiH₃ bond is concluded to be very difficult (vide infra). In **3**, ethylene is far from the Zr center with little lengthening of the C=C double bond. Actually, **3** is not very stable as compared to the reactant **1** + C₂H₄ (see below). From **3**, ethylene is inserted into the Zr−SiH₃ bond through transition state **TS₃₋₄ₐ**, to afford Cp₂Zr(H)(CH₂CH₂-SiH₃), **4**. In this **TS₃₋₄ₐ**, the SiH₃ group considerably changes its direction toward ethylene with little lengthening of the Zr−Si distance. The Zr−C distance is still 2.889 Å, which is considerably longer than that of the product **4**. This feature is quite different from that observed in the ethylene insertion into Pt−H, Pt−SiH₃, Rh−H, Rh−SiH₃, Ni−CH₃, Cu−H, and Cu−CH₃ bonds in which the metal−alkyl bond is almost formed at the transition state.[13,14,40,41] One of the plausible reasons is that ethylene approaches the Zr center with difficulty because of the steric repulsion with two Cp ligands; note that two Cp

(40) Sakaki, S.; Musashi, Y. *Inorg. Chem.* **1995**, *34*, 1914.
(41) Tomita, T.; Takahama, T.; Sugimoto, M.; Sakaki, S. *Organometallics* **2002**, *21*, 4138.

Table 1. Activation Barrier (E_a) and Energy of Reaction (ΔE) of the Ethylene Insertion into the Zr−H and Zr−SiH₃ Bonds (kcal/mol)

Ethylene Insertion into the Zr−H Bond		
	$E_a{}^a$	ΔE^b
DFT	2.1	−24.6
MP2	5.8	−41.4
MP3	3.5	−32.6
MP4(DQ)	3.2	−32.7
MP4(SDQ)	3.0	−34.2

Ethylene Insertion into the Zr−SiH₃ Bond			
	BE^c	$E_a{}^a$	ΔE^b
DFT	2.4	41.0	−17.5 (−19.1)
MP2	−5.5	35.9	−29.3 (−23.8)
MP3	−2.6	47.8	−24.5 (−21.9)
MP4(DQ)	−2.5	48.2	−23.8 (−21.3)
MP4(SDQ)	−2.6	44.5	−24.3 (−21.7)

a The energy difference between the reactant complex and the transition state. *b* The energy difference between the reactant and the product. A negative value means that the reaction is exothermic. *c* The energy difference between the reactant complex and the reactants. A negative value means that the reactant complex is more stable than the reactants.

ligands open toward the H and SiH₃ groups bound with the Zr center but ethylene must approach the Zr center from the direction in which two Cp ligands do not open (see Figure 1).

As shown in Table 1, the binding energy (BE) of the reactant complex, the activation barrier (E_a), and the energy of reaction (ΔE) are calculated with various methods, where the BE value is defined as the energy difference between the reactant complex and the reactants, the E_a value is the energy difference between the transition state and the reactant complex, and the ΔE value is the energy difference between the product and the reactants. Apparently, all of the computational methods employed here show that the ethylene insertion into the Zr−H bond takes place with nearly no barrier and significantly large exothermicity. This result agrees well with the previous theoretical work of hydrozirconation.[38] On the other hand, all of the computational methods here indicate that the ethylene insertion into the Zr−SiH₃ bond requires a very large activation barrier. This result is consistent with the experimental result that the alkene insertion into the Zr−silyl and Hf−silyl bonds needs a very long reaction time.[20] In general, the ethylene insertion into the M−SiH₃ bond needs a larger activation barrier than does the insertion into the M−H bond because the SiH₃ group has a directional sp³ valence orbital but the H(hydride) ligand has a spherical 1s orbital.[13,14] Thus, it should be clearly concluded that the Cp₂Zr-catalyzed hydrosilylation of alkene does not proceed through the modified Chalk−Harrod mechanism.

We wish to mention the reliability of the computational method here. The DFT method provides a considerably smaller ΔE value than does the MP4(SDQ) method in both insertion reactions, while a similar activation barrier was calculated from both the DFT and the MP4(SDQ) methods. Because the ΔE value converges upon going from MP2 to MP4(SDQ), the MP4-(SDQ) method is considered reliable. Also, the binding energy (BE) of the reactant complex **3** was calculated to be positive by the DFT method, while the MP2−MP4(SDQ) methods provide −3 to −6 kcal/mol of the BE value. This is probably because the DFT method with the B3LYP functional does not incorporate well the dispersion energy[42] and underestimates the binding energy. Thus, the MP4(SDQ) method is better than the DFT method for the ethylene insertion reactions. However, we

could not perform MP4(SDQ) calculations in the product release steps due to the large size of the system. We will present our discussion based on the DFT method with some caution, which will be described below in more detail.
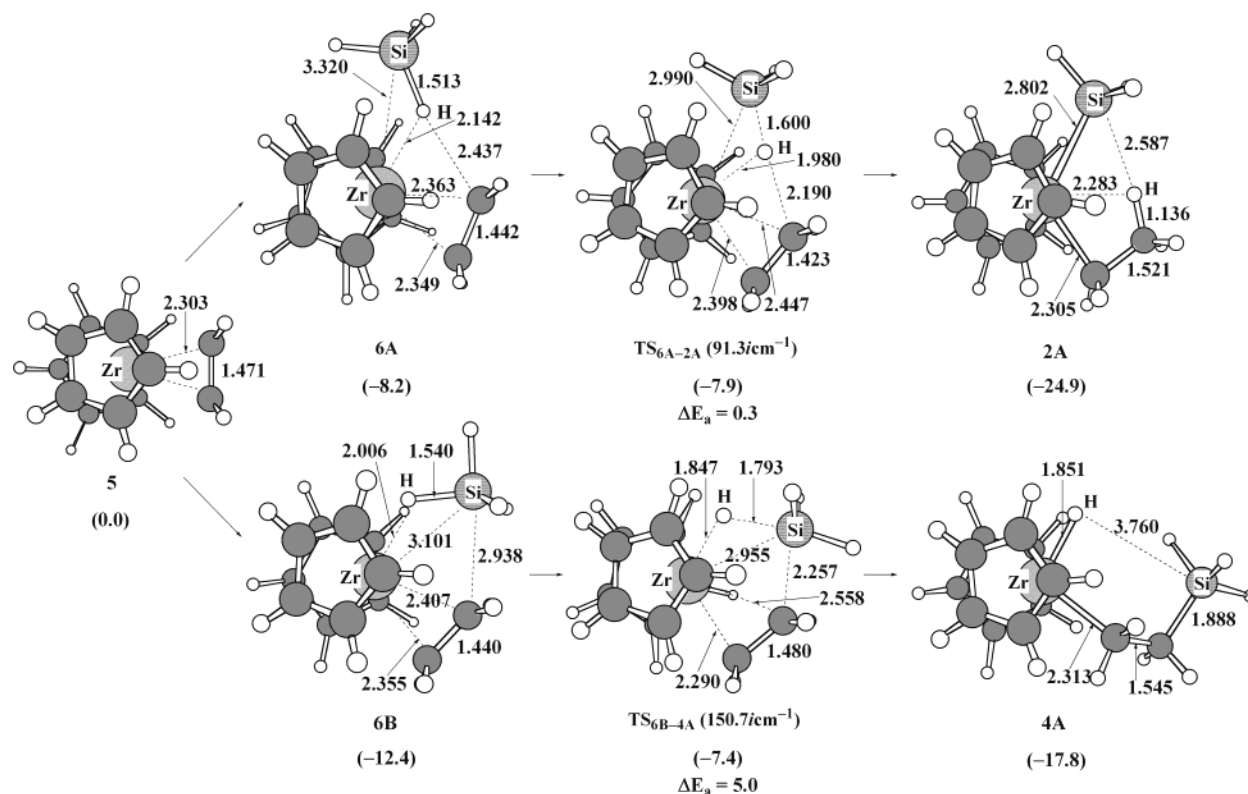
Reaction between Cp₂Zr(C₂H₄) and SiH₄. As shown in Figure 2, silane, SiH₄, approaches the Zr center of Cp₂Zr(C₂H₄), **5**, to afford two kinds of reactant complexes, Cp₂Zr(C₂H₄)(SiH₄), **6A** and **6B**, where the H atom of SiH₄ takes a position close to ethylene in **6A** and the SiH₃ group takes a position close to ethylene in **6B**. In these reactant complexes, the Zr−ethylene distance becomes longer than in **5** and the C=C double bond becomes shorter to 1.442 and 1.440 Å in **6A** and **6B**, respectively, than that (1.471 Å) of **5**. These geometrical changes suggest that the interaction between ethylene and the Zr center becomes weak by the interaction between SiH₄ and the Zr center. Actually, the interaction between the Zr center and SiH₄ is considerably strong, which will be discussed below in more detail. Also, the Si−H bonds of **6A** and **6B** are slightly longer than that of free SiH₄ by ca. 0.02 and 0.04 Å, respectively, and the Zr−H distance is rather similar to the Zr−hydride bond distance. These features resemble well those of the complex that involves an agostic interaction between the metal center and the Si−H bond.[13,14] This suggests that these reactant complexes are formed through the interaction similar to the agostic interaction. Because the Si−H bond of **6B** is longer than that of **6A**, the interaction between the Zr center and SiH₄ in **6B** is stronger than that in **6A**, which is consistent with the fact that the distance between the Zr center and ethylene is shorter in **6A** than that in **6B**.

In the transition state **TS₆ₐ₋₂ₐ** leading to **2A**, the H atom is moving from the Si atom to ethylene, where the Si−H distance somewhat lengthens by ca. 0.1 Å but the C−H distance is still long (2.190 Å). The Zr−C distance is only 0.093 Å longer than that of the product **2A**. These features indicate that the Zr−alkyl bond is already formed in this transition state but the C−H bond is not formed yet and the Si−H bond is still kept. One of the important geometrical features is that the Zr−H distance (1.980 Å) is similar to the Zr−hydride bond of **1**. This indicates that a considerable bonding interaction exists between the Zr center and the H atom that is moving from the Si atom to ethylene, while the Si−H bond is almost kept in the transition state.

In the other transition state **TS₆ᵦ₋₄ₐ** leading to **4A**, the Si−H distance becomes considerably longer than that of free SiH₄, and the Si−C distance is about 0.37 Å longer than that of the product **4A**. The Zr−C distance (2.290 Å) is almost the same as that of **4A**. These features again indicate that the formation of the Zr−alkyl bond is already completed in the transition state but the formation of the Si−C bond is on the way. An important feature of this transition state is that the Si atom takes a five-coordinate structure. This suggests that the Si atom takes hypervalency in the transition state. Because of this hypervalency, this reaction easily proceeds, as will be discussed below in more detail.

The BE, E_a, and ΔE values are listed in Table 2. Apparently, all of the calculations show that the coupling reaction between Cp₂Zr(C₂H₄) and SiH₄ easily occurs with either nearly no barrier to afford **2A** or a very small barrier to afford **4A**. It is also

(42) For instance: (a) Kristhan, S.; Pulay, P. *Chem. Phys. Lett.* **1994**, *229*, 175. (b) Perez-Jorda, J. M.; Becke, A. D. *Chem. Phys. Lett.* **1995**, *233*, 134.

Figure 2. Geometry changes in the coupling reaction between Cp$_2$Zr(C$_2$H$_4$), **5**, and SiH$_4$. Bond lengths are in angstroms. In parentheses are the relative energies (kcal/mol) to **5**, where the DFT(B3LYP)/BS-II method was employed.

Table 2. The Stabilization Energy (BE)^a of the Reactant Complex, the Activation Barrier (E_a),^{b} and the Energy of Reaction (ΔE)^c in the Reaction between Cp$_2$Zr(C$_2$H$_4$) and SiH$_4$ (in kcal/mol)

Reaction Leading to Cp$_2$Zr(C$_2$H$_5$)(SiH$_3$), **2A**			
	BE	E_a	ΔE
DFT	−8.2	0.3	−24.9 (−16.7)
MP2	−19.9	1.8	−36.4 (−16.5)
MP3	−15.3	1.4	−32.5 (−17.2)
MP4(DQ)	−15.8	1.2	−33.3 (−17.8)
MP4(SDQ)	−16.6	0.8	−35.9 (−19.3)

Reaction Leading to Cp$_2$Zr(CH$_2$CH$_2$SiH$_3$)(H), **4A**			
	BE	E_a	ΔE
DFT	−12.4	5.0	−17.8 (−5.4)
MP2	−25.4	5.3	−24.2 (1.2)
MP3	−19.4	6.5	−24.4 (−5.0)
MP4(DQ)	−20.0	6.3	−24.4 (−4.4)
MP4(SDQ)	−21.2	4.9	−26.0 (−4.8)

^{a} The energy stabilization of the reactant complex relative to the sum of Cp$_2$Zr(C$_2$H$_4$) and SiH$_4$. A negative value represents that the reactant complex is more stable than the reactants. ^{b} The energy difference between the reactant complex and the transition state. ^{c} The energy difference between the product and the sum of reactants. A negative value represents that the reaction is exothermic.

noted that the BE value is considerably large in MP2−MP4-(SDQ) computations. This means that the interaction between the Zr center and SiH$_4$ is considerably strong, as mentioned above. Although the similar activation barrier is calculated with all of the methods adopted here, several discrepancies are observed between the DFT method and the others. For instance, the DFT method underestimates the BE value, as compared to the other methods. This is because the DFT method cannot incorporate well the dispersion energy that plays an important role in the interaction between the σ-bond and the transition

metal center, as described above.[42] The energy of reaction (ΔE) calculated by the DFT method is much smaller than that calculated with the MP2−MP4 methods such as that of ethylene insertion reactions (see below). The ΔE value converges to −33 to −35 kcal/mol in the reaction leading to **2A** and −24 to −25 kcal/mol in the reaction leading to **4A** upon going from MP2 to MP4(SDQ). Thus, the MP4(SDQ) method is considered reliable for estimating the ΔE value, but the DFT method underestimates the ΔE value in the coupling reaction between Cp$_2$Zr(C$_2$H$_4$) and SiH$_4$. On the other hand, all of the methods here including the DFT method provide a similar ΔE value relative to the reactant complex. These results suggest that the DFT method underestimates the dispersion energy in all of the species here to a similar extent and the energy change after the reactant complex is reliably calculated with the DFT method, in a practical sense.

It is of considerable interest to clarify the important interaction in this coupling reaction. The contour maps of HOMO at the transition states **TS$_{6A−2A}$** and **TS$_{6B−4A}$** are shown in Figure 3. Both contour maps clearly display that the strong π-back-donating interaction is formed between the d$_\pi$ orbital of Zr and the π* orbital of ethylene. One of the important features here is that the Si−H σ* orbital starts to mix into the π-back-donating orbital in a bonding way in these transition states; this orbital mixing leads to the Si−H bond fission and either formation of C−H and Zr−SiH$_3$ bonds in **TS$_{6A−2A}$** or formation of C−Si and Zr−H bonds in **TS$_{6B−4A}$**, as is schematically shown in Scheme 6. Thus, it is reasonably concluded that the strong π-back-donation is necessary to achieve this coupling reaction. Actually, Cp$_2$Zr(C$_2$H$_4$) involves much stronger π-back-donation than does PtCl$_2$(PH$_3$)(C$_2$H$_4$), as follows: The NBO charge of C$_2$H$_4$ is −0.709e in Cp$_2$Zr(C$_2$H$_4$) but −0.137e in PtCl(PH$_3$)$_2$-

(A) TS$_{6A-2A}$ **(B) TS$_{6B-4A}$**
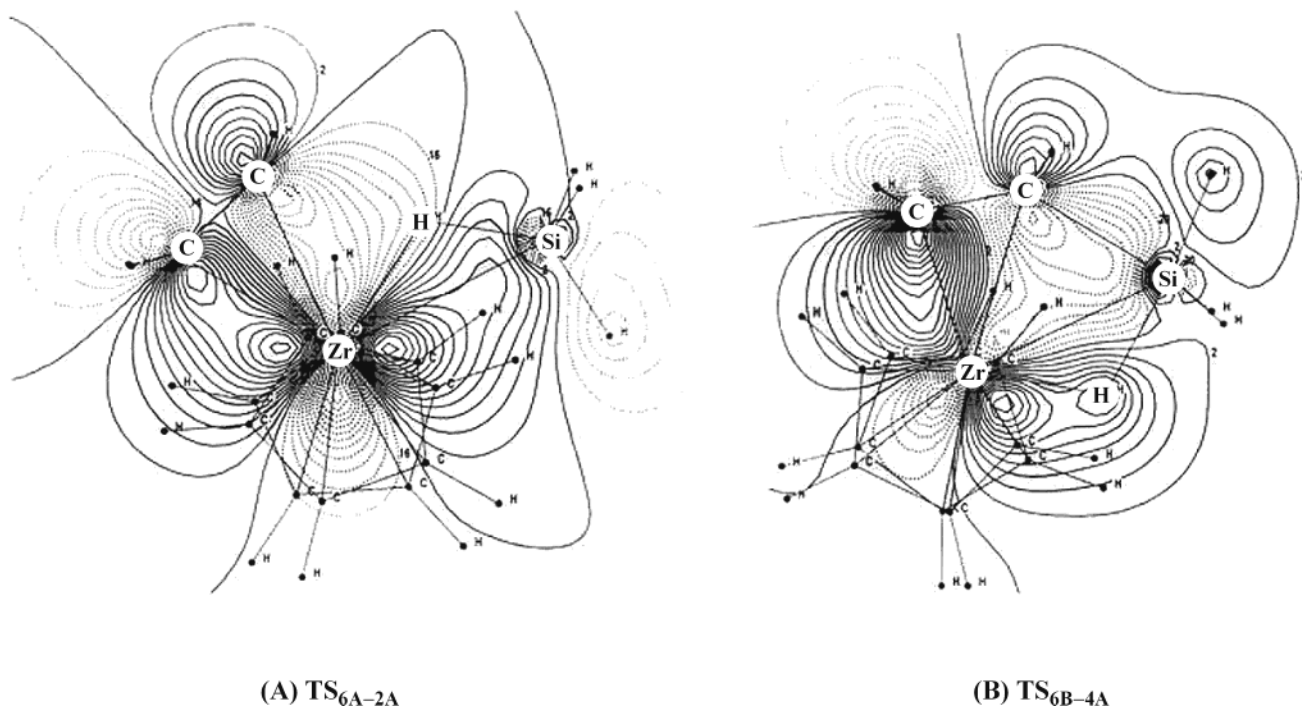
Figure 3. Contour maps of HOMOs of the transition states of the coupling reaction between Cp₂Zr(C₂H₄), **5**, and SiH₄. Contour values are 0.0, ±0.0125, ±0.025, ±0.0375, and so on (in e$^{1/2}$ au$^{-3/2}$), where the HF/BS-II method was employed.

Scheme 6

Scheme 7
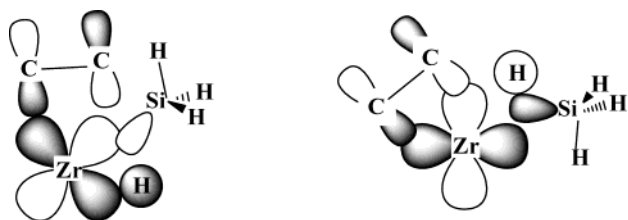
(C₂H₄), where these populations were calculated with the DFT/BS-II method.[43] The very strong d$_\pi$-π* interaction between the Zr center and C₂H₄ results from the fact that Cp₂Zr has a d orbital at much higher energy than does PtCl₂(PH₃), as was previously shown by us.[44] Because of the very strong π-back-donation interaction, the Zr(C₂H₄) moiety in Cp₂Zr(C₂H₄) is understood in terms of a metallocyclopropane ring and the coupling reaction is characterized to be σ-bond metathesis between the Zr−C bond of metallocyclopropane and the Si−H bond, as shown in Scheme 7. The high energy of the d orbital of Cp₂Zr is also responsible for new reaction courses of the product release step in the Cp₂Zr-catalyzed hydrosilylation of alkene, as will be discussed below.

At the end of this section, we wish to mention the relations between the HOMO and the Zr−H bonding interaction observed in **TS$_{6A-2A}$** and between the HOMO and the hypervalency of the Si atom observed in **TS$_{6B-4B}$**. In the HOMO of **TS$_{6A-2A}$**, the H atom is involved in the positive phase of the d$_\pi$ orbital of
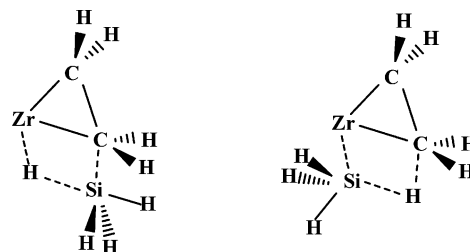
Zr into which the π* orbital of ethylene overlaps in a bonding way. This means that the bonding interaction exists between the Zr center and the H atom, which is consistent with the Zr−H distance that is similar to the Zr−hydride bond distance. In the HOMO of **TS$_{6B-4B}$**, the bonding interaction between the Si atom and the C atom of ethylene is clearly observed. Thus, the Si atom takes a five-coordinate system, as discussed above. More important is that the π-back-donation of the Zr−C₂H₄ moiety provides negative charge on the C atom because the negatively charged species tends to take an axial position of the hypervalent Si atom. Again, it is clearly shown that the very strong π-back-donation of the Zr−C₂H₄ moiety is necessary for this hypervalency.

Si−C Reductive Elimination of Cp₂Zr(SiH₃)(CH₂CH₃), 2. The reductive elimination was experimentally proposed as the final step of the catalytic cycle in general.[1] Although **2A** is directly formed through the ethylene insertion into the Zr−H bond and the coupling reaction between Cp₂Zr(C₂H₄) and SiH₄, the Si−C reductive elimination of **2A** is considered difficult because one of the H atoms of the ethyl group takes an unfavorable position for the approach of the SiH₃ group to the ethyl group. We optimized the rotation isomers, as shown in Figure 4. The rotation isomers **2B** and **2C** are slightly more stable than **2A**, where **2B** possesses the ethyl group almost perpendicular to the Si−Zr−C plane and **2C** possesses the ethyl

(43) The effective core potentials and basis sets of the same quality as that of BS-I were used in the geometry optimization with the DFT(B3LYP) method; core electrons of Pt, P, and Cl atoms were replaced with the ECPs, and their valence electrons were represented with (311/311/21) and (21/21/1) sets, respectively.[26−28] Electron populations were evaluated with the same ECPs and better basis sets, (541/541/111) set for Pt, while the same basis sets were used for Cl and P.[26−28,31]

(44) Sakaki, S.; Takayama, T.; Sugimoto, M. *Organometallics* **2001**, *20*, 3896. In this work, the d orbital energy of Cp₂Zr is compared to that of Pt(PH₃)₂. The former is at much higher energy than the latter. The d orbital of PtCl₂(PH₃) is considered to be much lower than that of Pt(PH₃)₂.
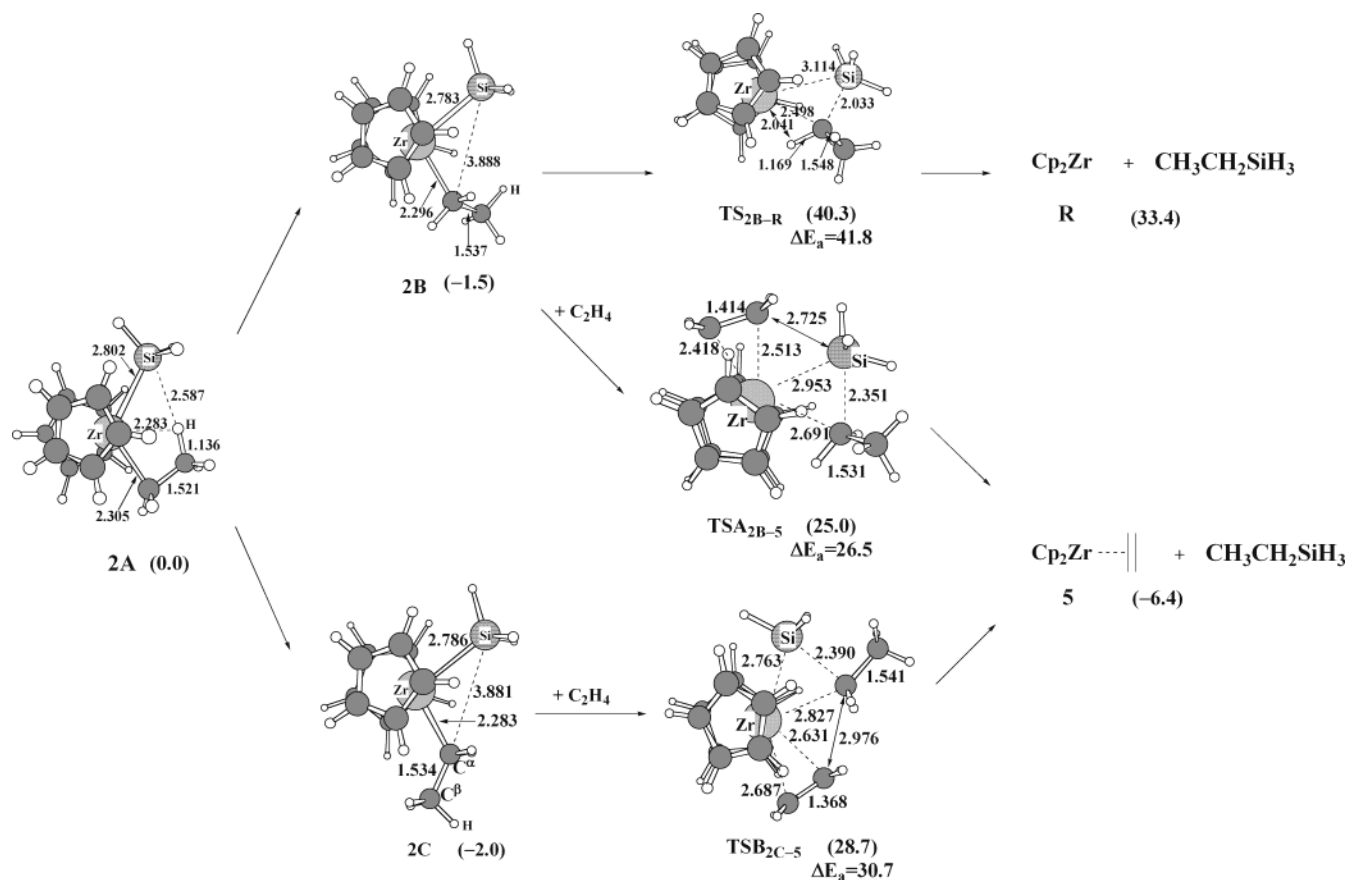
Figure 4. Geometry changes in the Si−C reductive elimination of $Cp_2Zr(C_2H_5)(SiH_3)$, **2**. Bond lengths are in angstroms. In parentheses are the relative energies (kcal/mol) to **2A**, where the DFT(B3LYP)/BS-II method was employed.

group on the Si−Zr−C plane but in the direction reverse from that of **2A**. The transition state of the rotation was not optimized here because such rotation easily occurs in general. The Si−C reductive elimination proceeds through the transition state **TS$_{2B-R}$**, to afford Cp_2Zr **R** and $CH_3CH_2SiH_3$ (see Figure 4). In **TS$_{2B-R}$**, the Zr−Si and Zr−C distances lengthen to 3.114 and 2.498 Å, respectively, while the Si−C distance is 2.033 Å, which is only 0.1 Å longer than that of the product. This transition state is product-like. Consistent with its geometry, the activation barrier and the endothermicity are very large (41.9 and 33.4 kcal/mol, respectively), where the activation barrier and the energy of reaction calculated with the DFT(B3LYP)/BS-II method are given hereafter because the MP2−MP4(SDQ) methods could not be applied to the product release step such as ethylene-assisted reductive elimination and metathesis (see below) because of their large size. It should be clearly concluded that this direct Si−C reductive elimination is very difficult. We stopped to optimize the transition state of the Si−C reductive elimination starting from **2B** and **2C**, considering the very large activation barrier and endothermicity of this reaction.

We then examined the ethylene-assisted Si−C reductive elimination leading to $Cp_2Zr(C_2H_4)$, **4**, and $CH_3CH_2SiH_3$, because our previous theoretical work showed that the coordination of ethylene decreased the activation barrier of the reductive elimination[13,14] and Ozawa et al. experimentally reported that alkyne accelerated the Si−C reductive elimination of $Pt(SiR_3)$-$(CH_3)(PR_3)_2$.[45] In this reaction, two kinds of transition states

(45) Ozawa, F.; Hikida, T.; Hayashi, T. *J. Am. Chem. Soc.* **1994**, *116*, 2844.

(**TSA$_{2B-5}$** and **TSB$_{2C-5}$**) were optimized, as shown in Figure 4; in **TSA$_{2B-5}$**, ethylene approaches the Zr center so as to push the SiH$_3$ group toward the ethyl group, while in **TSB$_{2C-5}$** ethylene approaches the Zr center so as to push the ethyl group toward the SiH$_3$ group. In **TSA$_{2B-5}$**, the Zr−Si distance moderately lengthens to 2.953 Å, but the direction of the SiH$_3$ group slightly changes toward the ethyl group. On the other hand, the Zr−C distance somewhat lengthens to 2.691 Å, and the alkyl group considerably changes its direction toward the SiH$_3$ group. The Si−C distance is 2.351 Å, which is considerably longer than that of the product. These features suggest that the Zr−SiH$_3$ bond is almost kept while the Zr−C bond fission and the Si−C bond formation are on the way in this transition state. The distance between ethylene and the Zr center is about 0.2 Å longer than that of $Cp_2Zr(C_2H_4)$, **5**, and the C=C distance is shorter than that of **5**. Although the ethylene coordination with the Zr center has not been completed yet in this transition state, ethylene is approaching the Zr center, and the Zr−ethylene distance indicates that the bonding interaction exists between the Zr center and ethylene. This bonding interaction contributes to the stabilization of the transition state.

In the other transition state **TSB$_{2C-5}$**, the Zr−Si distance is 2.763 Å, which is almost the same as that of **2C**, while the silyl group is changing its direction toward the ethyl group. The Zr−C distance considerably lengthens to 2.827 Å. The Si−C distance is 2.390 Å, which is considerably longer than the usual Si−C bond, and the ethyl group also changes its direction toward the SiH$_3$ group. These geometrical features indicate that the Zr−SiH$_3$ bond is still kept in this transition state while the Si−C
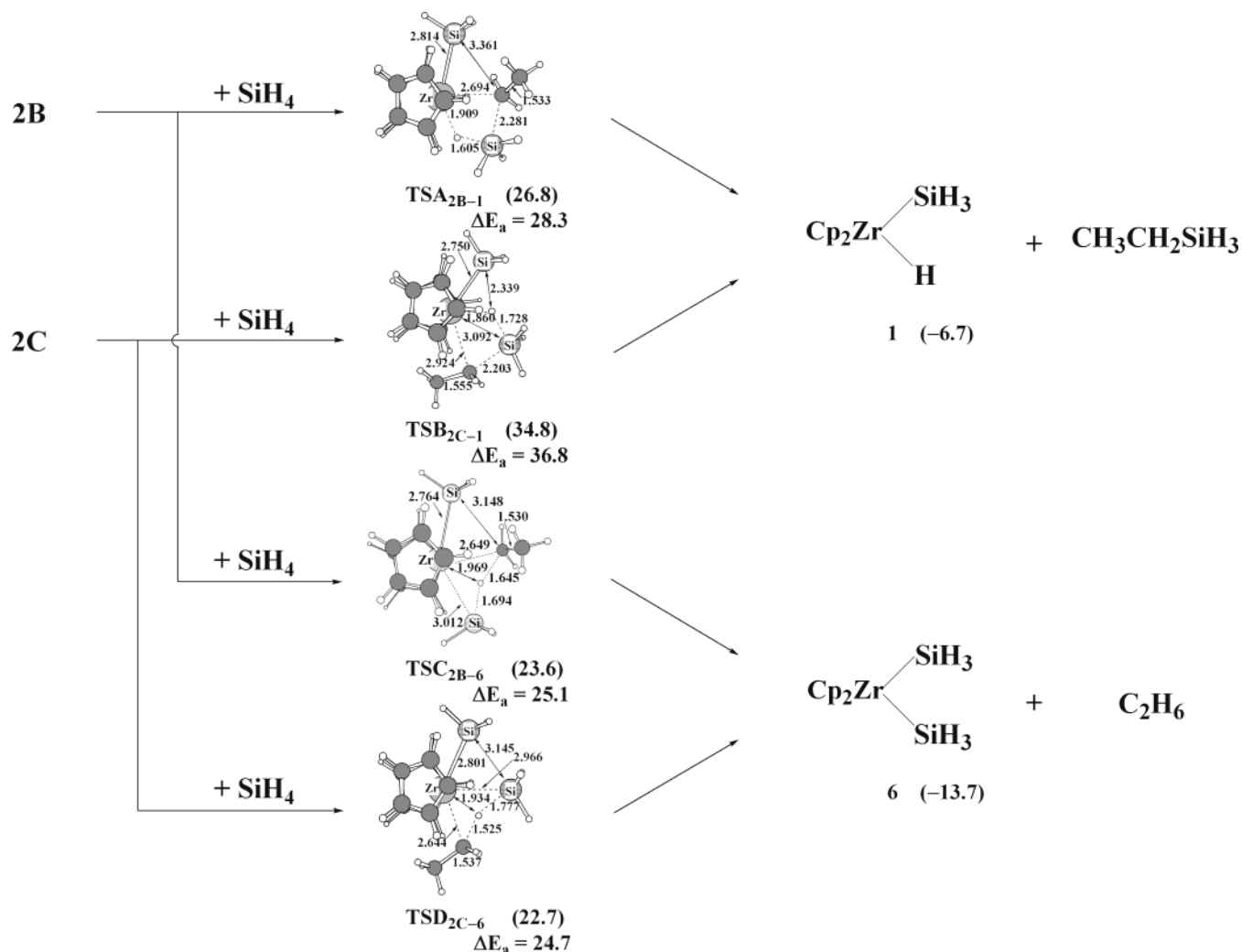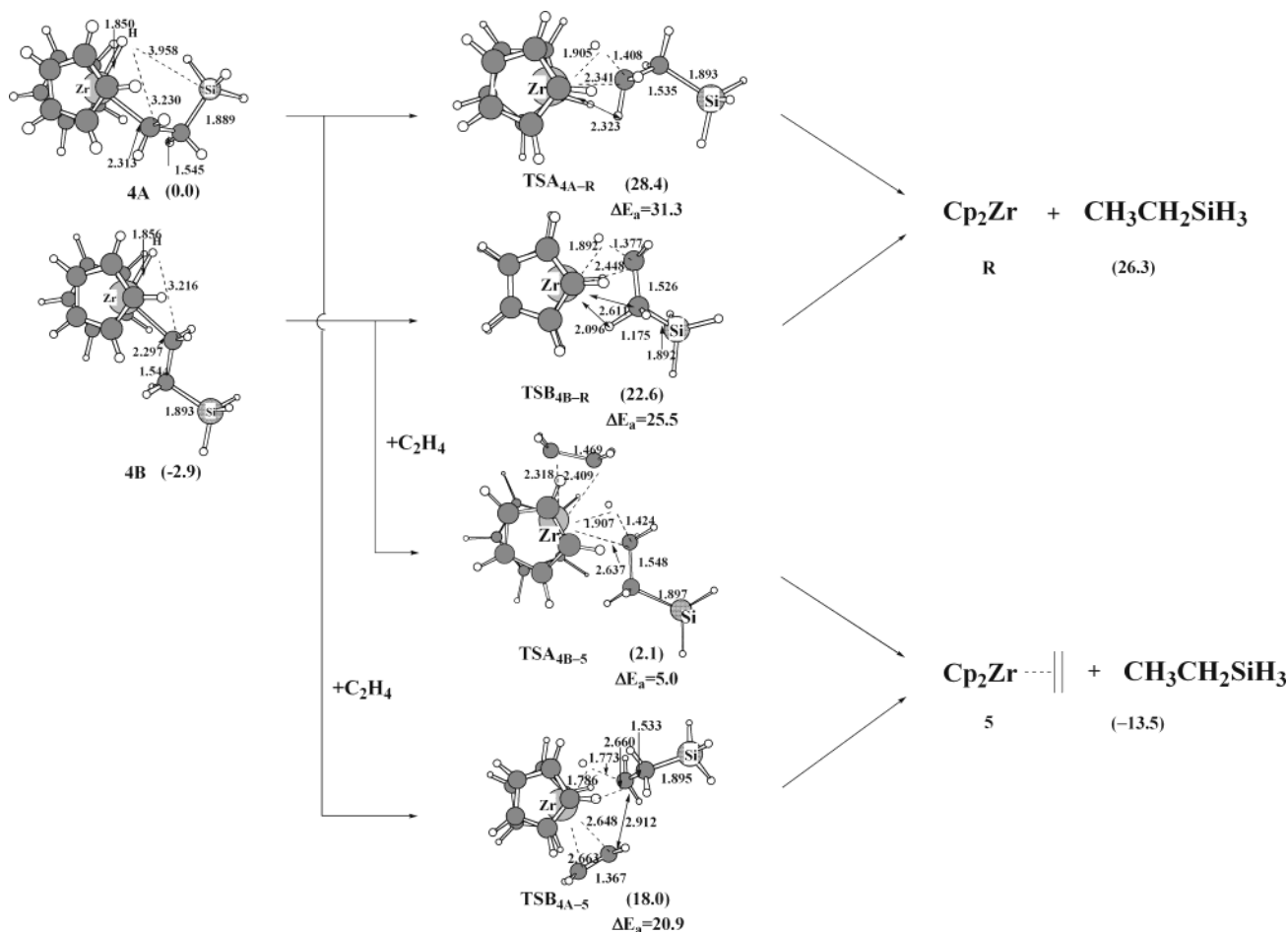
Figure 5. Geometry changes in the metathesis of $Cp_2Zr(C_2H_5)(SiH_3)$, **2**, with SiH_4. Bond lengths are in angstroms. In parentheses are the relative energies (kcal/mol) to **2A**, where the DFT(B3LYP)/BS-II method was employed.

bond formation and the Zr−C bond fission are on the way. An important difference between these two transition states is observed in the distance between the Zr center and ethylene; ethylene is closer to the Zr center in **TSA₂B−₅** than in **TSB₂C−₅**. This means that ethylene contributes more to the stabilization of **TSA₂B−₅** than that of **TSB₂C−₅**. As shown in Figure 4, this ethylene-assisted Si−C reductive elimination needs the activation barrier of 26.5 kcal/mol for the former transition state and the barrier of 30.2 kcal/mol for the latter transition state. These activation barriers are much smaller than that of the direct Si−C reductive elimination. Also, it is noted that the ethylene-assisted Si−C reductive elimination is considerably exothermic. From these results, it should be reasonably concluded that this Si−C reductive elimination is considerably accelerated by ethylene coordination.

Metathesis of Cp₂Zr(CH₂CH₃)(SiH₃), 2, with SiH₄. Cp₂-Zr(CH₂CH₃)(SiH₃), **2**, also undergoes metathesis with SiH_4, as shown in Figure 5. From **2B**, the metathesis takes place through **TSA₂B−₁** to afford $CH_3CH_2SiH_3$ with concomitant formation of $Cp_2Zr(H)(SiH_3)$, **1**. In this reaction, SiH_4 approaches the Zr center from the side of the ethyl group. In **TSA₂B−₁**, the Zr−H distance is 1.909 Å, which is almost the same as that of **1**, while the Si−H distance moderately lengthens to 1.605 Å and the SiH_3 moiety of SiH_4 is changing its direction toward the ethyl

group. The Zr−ethyl distance lengthens to 2.694 Å by ca. 0.39 Å, and the ethyl group is changing its direction toward the SiH_3 group. However, the Si−C distance is still 2.281 Å, which is somewhat longer than that of the product. From these geometrical features, it is reasonably concluded that the Zr−H bond formation is on the way but the Si−H bond is almost kept and the ethyl group is moving to the SiH_3 moiety of SiH_4 with a change in its direction toward SiH_4 in this transition state. The activation barrier is 28.3 kcal/mol, which is much smaller than that of the direct Si−C reductive elimination. This is because the Zr−SiH₃ bond is kept as it is in **2A** and **2B** and the Zr−H bonding interaction is almost formed in this transition state.

From **2C**, the metathesis proceeds through the transition state **TSB₂C−₁** to afford $Cp_2Zr(H)(SiH_3)$, **1**, and $CH_3CH_2SiH_3$. In this reaction, SiH_4 approaches the Zr center between the SiH_3 and ethyl groups. In **TSB₂C−₁**, the C−Si distance is 2.203 Å, and the Zr−ethyl distance lengthens to 2.924 Å. These geometrical features indicate that the Zr−ethyl bond is almost broken while the Si−C bond formation is on the way. The Zr−H distance is 1.860 Å, while the Si−H distance is 1.728 Å. Thus, the Si−H bond becomes somewhat weak in this transition state, while the Zr−H bond formation is almost completed. The activation barrier (36.7 kcal/mol) of **TSB₂C−₁** is considerably larger than that (28.3 kcal/mol) of **TSA₂B−₁**. However, a significant
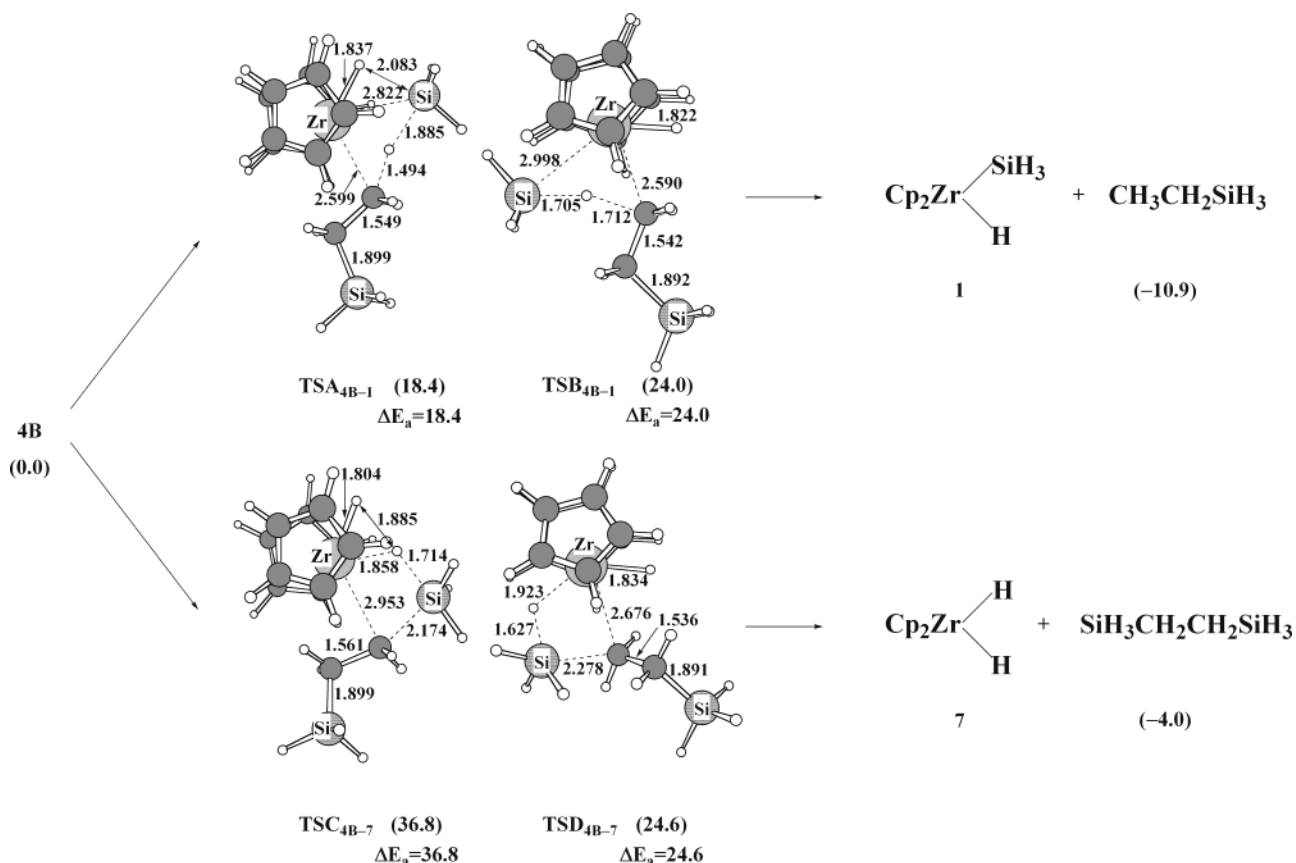
Figure 6. Geometry changes in the C−H reductive elimination of $Cp_2Zr(H)(CH_2CH_2SiH_3)$, **4**. Bond lengths are in angstroms. In parentheses are the relative energies (kcal/mol) to **4A**, where the DFT(B3LYP)/BS-II method was employed.

difference in geometry is not observed between **TSA₂B₋₁** and **TSB₂C₋₁** except for the position of the ethyl group. The difference in the E_a value between **TSA₂B₋₁** and **TSB₂C₋₁** would be attributed to the steric repulsion between the ethyl group and Cp ligands, as follows: The ethyl group must approach the Cp ligands to change its direction toward SiH₄ in **TSB₂C₋₁**, as shown in Figure 5, while the ethyl group is distant from the Cp ligands in **TSA₂B₋₁**. As a result, the steric repulsion between the ethyl group and Cp ligands is larger in **TSB₂C₋₁** than that in **TSA₂B₋₁**.

If the orientation of SiH₄ becomes reverse in **TSA₂B₋₁** and **TSB₂C₋₁**, $Cp_2Zr(SiH_3)_2$ and C_2H_6 are formed as products. These transition states, **TSC₂B₋₆** and **TSD₂C₋₆**, were optimized, as shown in Figure 5, and the activation barrier of **TSC₂B₋₆** was estimated to be 25.1 kcal/mol and that of **TSD₂C₋₆** was 24.7 kcal/mol (the DFT/BS-II method). These activation barriers are slightly smaller than that of **TSA₂B₋₁**. Thus, the hydrosilylation would compete with the hydrogenation. Consistent with these computational results, Takahashi and his collaborators reported that hydrosilane was completely consumed but the yield of hydrosilylated product did not reach 100%, while byproduct was not clearly described.[15] If the bulky substituent is introduced in the Si atom instead of the H atom, **TSC₂B₋₆** and **TSD₂C₋₆** would become more unstable, because $Cp_2Zr(SiR_3)_2$ becomes less stable due to the steric repulsion of two bulky silyl groups. H_2SiPh_2 was used in the experimental work.[15] Thus, the

theoretical calculation with more realistic hydrosilane would facilitate the hydrosilylation as compared to the hydrogenation.

C−H Reductive Elimination of $Cp_2Zr(H)(CH_2CH_2SiH_3)$, 4. Although **4A** is directly formed through the ethylene insertion into the Zr−SiH₃ bond and the coupling reaction between **5** and SiH₄, we optimized the rotation isomer **4B**, which is slightly more stable than **4A**, as shown in Figure 6. The transition state of the rotation around the C−C bond was not optimized here because this rotation is expected to occur easily. The C−H reductive elimination takes place through two kinds of transition states, **TSA₄A₋R** and **TSB₄B₋R**, to afford Cp_2Zr **R** and CH₃-CH₂SiH₃, as shown in Figure 6. In the transition state **TSA₄A₋R**, the Zr−H distance slightly lengthens to 1.905 Å by only 0.045 Å, and the Zr−C distance slightly lengthens to 2.341 Å by only 0.028 Å. These bond lengths suggest that the Zr−H and Zr−C bonds are almost kept in **TSA₄A₋R**. On the other hand, the C−H distance of 1.408 Å suggests that the C−H bond formation is on the way. In the other transition state **TSB₄B₋R**, the Zr−H distance (1.892 Å) is similar to that of **TSA₄B₋R**, while the C−H distance is slightly shorter and the Zr−C distance is somewhat longer than those of **TSA₄B₋R**. The E_a values, 25.5 kcal/mol for **TSB₄B₋R** and 31.2 kcal/mol for **TSA₄B₋R**, are much smaller than that (41.9 kcal/mol) of the direct Si−C reductive elimination. However, the C−H reductive elimination is significantly endothermic like that of the direct Si−C reductive elimination. Thus, the direct C−H reductive elimination is difficult, too, like

Figure 7. Geometry changes in the metathesis of Cp₂Zr(H)(CH₂CH₂SiH₃), **4**, with SiH₄. Bond lengths are in angstroms. In parentheses are the relative energies (kcal/mol) to **4B**, where the DFT(B3LYP)/BS-II method was employed.

the direct Si−C reductive elimination. Here, we omitted further discussion of the direct C−H reductive elimination.

We then examined the ethylene-assisted C−H reductive elimination. As shown in Figure 6, this ethylene-assisted C−H reductive elimination takes place through the transition state **TSA₄ᵦ₋₅**, to afford Cp₂Zr(C₂H₄), **5**, and CH₃CH₂SiH₃. In **TSA₄ᵦ₋₅**, ethylene approaches the Zr center from the side of the H ligand. The Zr−H distance moderately lengthens, while the Zr−C distance considerably lengthens. The C−H distance is 1.424 Å, and the alkyl group is changing its direction toward the H ligand. The Zr−ethylene distance is slightly longer than that in Cp₂Zr(C₂H₄), which indicates that ethylene coordination considerably contributes to the stabilization of this transition state. As a result, the activation barrier (5.0 kcal/mol) is very small. Also, it should be noted that the C−H reductive elimination becomes remarkably exothermic in the presence of ethylene. The other transition state **TSB₄ₐ₋₅** was also optimized. In this transition state, the Zr−H distance little lengthens, while the Zr−C distance considerably lengthens. The C−H distance is still 2.773 Å, and ethylene is much further away from the Zr center. These geometrical features suggest that the Zr−H bond is almost kept while the Zr−alkyl bond fission and the formation of the ethylene coordinate bond are on the way. The activation barrier (20.9 kcal/mol) is smaller than that of the direct C−H reductive elimination but larger than that for **TSA₄ᵦ₋₅**. Thus, it should be concluded that the ethylene-assisted C−H reductive elimination easily occurs through **TSA₄ᵦ₋₅** with a moderate activation barrier and considerable exothermicity.

Metathesis of Cp₂Zr(H)(CH₂CH₂SiH₃), 4, with SiH₄. The other possible reaction course is metathesis of Cp₂Zr(H)(CH₂-

CH₂SiH₃), **4**, with SiH₄. This metathesis proceeds through two kinds of transition states, **TSA₄ᵦ₋₁** and **TSB₄ᵦ₋₁**, to afford Cp₂-Zr(H)(SiH₃), **1**, and CH₃CH₂SiH₃, as shown in Figure 7. In one transition state **TSA₄ᵦ₋₁**, SiH₄ approaches the Zr center between the H and CH₂CH₂SiH₃ ligands. The Si−H distance considerably lengthens to 1.885 Å by 0.39 Å, and the Zr−Si distance is 2.822 Å, which is almost the same as that of Cp₂Zr(H)(SiH₃). However, the C−H distance is still long (1.494 Å), and the Zr−C distance somewhat lengthens to 2.599 Å by 0.286 Å. These geometrical features indicate that the Zr−Si bond is already formed but the Zr−alkyl bond is weakened, and the H atom is moving from the SiH₃ group to the alkyl group. This transition state is essentially the same as that of heterolytic C−H σ-bond activation of benzene by Pd(II) complex.[46] In the other transition state **TSB₄ᵦ₋₁**, SiH₄ approaches the Zr center from the side of the alkyl group. In this transition state, the Zr−Si distance is somewhat longer and the Si−H distance is somewhat shorter than those of **TSA₄ᵦ₋₁**, while the C−H distance is somewhat longer than that of **TSA₄ᵦ₋₁**. The H atom is moving from the SiH₃ group to the alkyl group in this transition state, too, like that in **TSA₄ᵦ₋₁**.

The activation barrier of **TSA₄ᵦ₋₁** is evaluated to be 18.4 kcal/mol, and that of **TSB₄ᵦ₋₁** is 24.0 kcal/mol. The exothermicity is considerably large (13.8 kcal/mol). It should be concluded here that the metathesis of **4** with SiH₄ takes place much more easily than the direct C−H reductive elimination.

Although the geometrical features are similar in both transition states, the activation barrier of **TSB₄ᵦ₋₁** is somewhat larger

(46) Biswas, B.; Sugimoto, M.; Sakaki, S. *Organometallics* **2000**, *19*, 3895.
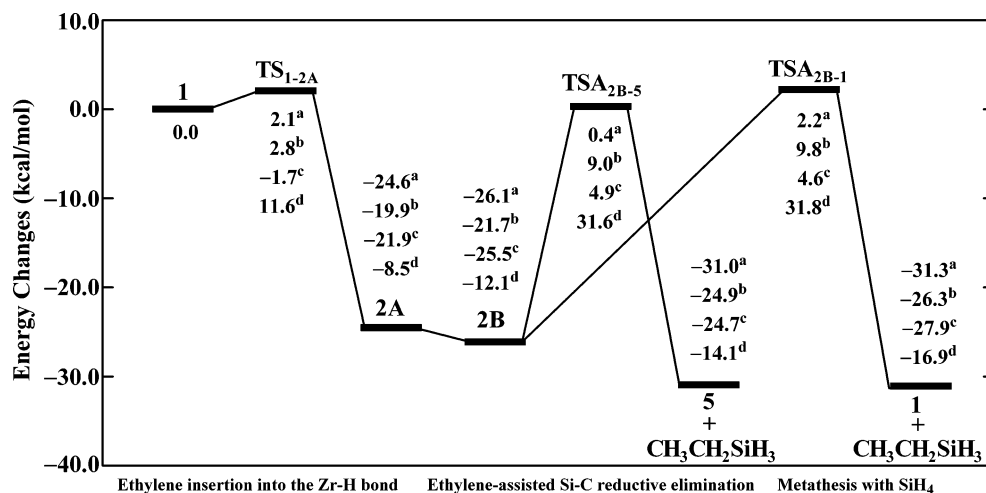
Figure 8. Energy changes in the catalytic cycle including the ethylene insertion into the Zr–H bond followed by either the ethylene-assisted Si–C reductive elimination or the metathesis with SiH$_4$ (kcal/mol unit). (a) Total energy changes without correction of the zero-point energy. (b) Total energy changes with correction of the zero-point energy. (c) Gibbs free energy change ($G°$) at 298 K, where only vibration movements are taken into the estimation of the thermal energy and entropy. (d) Gibbs free energy change ($G°$) at 298 K in the gas-phase reaction, where translation, rotation, and vibration movements are taken into the estimation of the thermal energy and entropy.

than that of **TSA$_{4B-1}$**. This difference is interpreted in terms of the position of SiH$_4$. In **TSB$_{4B-1}$**, SiH$_4$ takes a position near to the Cp ligands, as shown in Figure 7; note that two Cp ligands open in the direction to the H(hydride) and CH$_2$CH$_2$SiH$_3$ ligands but SiH$_4$ must approach the Zr center from the direction to which two Cp ligands close. This geometry gives rise to the steric repulsion between SiH$_4$ and two Cp ligands. In **TSA$_{4B-1}$**, on the other hand, SiH$_4$ approaches the Zr center from the direction to which two Cp ligands open. As a result, the activation barrier of **TSA$_{4B-1}$** is smaller than that of **TSB$_{4B-1}$**.

If the orientation of silane becomes reverse to those in **TSA$_{4B-1}$** and **TSB$_{4B-1}$**, then different products, Cp$_2$Zr(H)$_2$ and SiH$_3$CH$_2$CH$_2$SiH$_3$, would be produced. We optimized such transition states, **TSC$_{4B-7}$** and **TSD$_{4B-7}$**, as shown in Figure 7. The activation barrier of **TSC$_{4B-7}$** is evaluated to be 36.8 kcal/mol and that of **TSD$_{4B-7}$** is 24.6 kcal/mol, being larger than that of **TSA$_{4B-1}$**. Thus, Cp$_2$Zr(H)$_2$ and SiH$_3$CH$_2$CH$_2$SiH$_3$ would not be formed in the Cp$_2$Zr-catalyzed hydrosilylation of alkene.

Energy Changes along the Catalytic Cycle. Summarizing the above results, the catalytic cycle including ethylene insertion into the Zr–SiH$_3$ bond should be excluded because this insertion needs the very large E_a value and the very large activation free energy ($\Delta G°‡$), as shown above (see also Supporting Information Figure S-9 (B)). Also, the direct Si–C reductive elimination of Cp$_2$Zr(C$_2$H$_5$)(SiH$_3$) and the direct C–H reductive elimination of Cp$_2$Zr(H)(CH$_2$CH$_2$SiH$_3$) need the considerably large E_a and $\Delta G°‡$ values with considerably large endothermicity (see above and Supporting Information Figure S-9). Thus, the catalytic cycles including these elementary processes are excluded from the discussion. Remaining catalytic cycles are the ethylene insertion into the Zr–H bond followed by either ethylene-assisted Si–C reductive elimination or metathesis with SiH$_4$, and the coupling reaction between Cp$_2$Zr(C$_2$H$_4$) and SiH$_4$ followed by ethylene-assisted C–H reductive elimination, ethylene-assisted Si–C reductive elimination, or metathesis with SiH$_4$. The energy changes along these catalytic cycles are shown in Figures 8–10. In these figures, we present the activation barrier (E_a) and the energy of reaction (ΔE) calculated by the DFT(B3LYP)/BS-II method with and without correction of the

zero-point energy. The free energy changes at 298 K are also shown in these figures, where thermal energy and entropy were evaluated either with consideration of translation, rotation, and vibration movements or with only consideration of vibration movements.[35] Because the DFT(B3LYP) method tends to underestimate the energy of reaction, as was described above, the ethylene insertion and the coupling reaction are much more exothermic by about 8–10 kcal/mol than those shown in Figures 8–10. However, the underestimation of the reaction energy does not interfere with the discussion of the reaction course, because the exothermicity of each elementary step is considerably large and we do not need to take into consideration the reverse reaction in each elementary step. Thus, the correct discussion of the reaction mechanism can be presented here based on the DFT-calculated E_a values.

As discussed above, both Cp$_2$Zr(H)(SiH$_3$), **1**, and Cp$_2$Zr-(C$_2$H$_4$), **5**, can play the role of the active species, if they are of similar stability. If **1** was much more stable than **5**, we needed to exclude **5** from the active species and vice versa. Thus, we must investigate the relative stabilities of **1** and **5**, first. All of the computational methods here indicate that the energy of reaction of eq 2 is small: 0.3 kcal/mol with the DFT/BS-II method, and -5.1, -0.1, 0.6, and 1.7 kcal/mol with the MP2/BS-II, MP3/BS-II, MP4(DQ)/BS-II, and MP4(SDQ)/BS-II methods, respectively. The free energy change of this reaction is also small (+3.2 kcal/mol at 298 K).

$$\text{Cp}_2\text{Zr(H)(SiH}_3) \ \mathbf{1} + \text{C}_2\text{H}_4 \rightarrow \text{Cp}_2\text{Zr(C}_2\text{H}_4) \ \mathbf{5} + \text{SiH}_4 \quad (2)$$
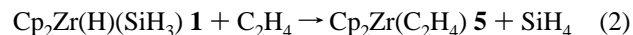
Thus, both Cp$_2$Zr(H)(SiH$_3$), **1**, and Cp$_2$Zr(C$_2$H$_4$), **5**, can play the role of the active species.

Starting from **1**, the ethylene insertion into the Zr–H bond occurs with the very small E_a value of 2.1 (2.8) kcal/mol and the considerably large ΔE value of -24.6 (-19.9) kcal/mol, to afford Cp$_2$Zr(CH$_2$CH$_3$)(SiH$_3$), **2**, as shown in Figure 8, where the E_a and ΔE values with zero-point energy correction are in parentheses and those values without zero-point energy correction are out of parentheses hereafter. The activation free energy ($\Delta G°‡$) of this insertion is moderately large (11.6 kcal/mol) in
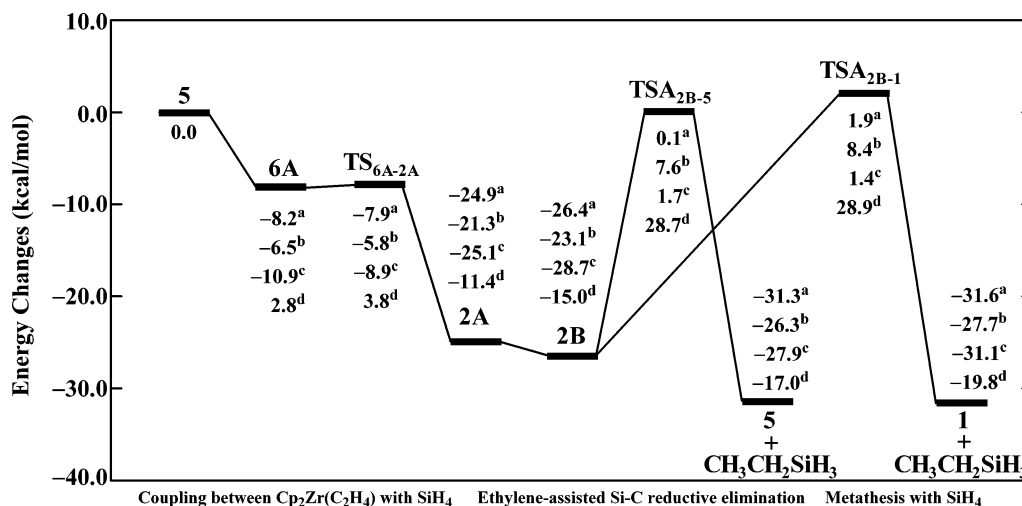
Figure 9. Energy changes in the catalytic cycle including the coupling reaction of $Cp_2Zr(C_2H_4)$ with SiH_4, to afford $Cp_2Zr(C_2H_5)(SiH_3)$, followed by either the ethylene-assisted Si−C reductive elimination or the metathesis with SiH_4 (kcal/mol unit). (a) Total energy changes without zero-point energy. (b) Total energy changes with correction of the zero-point energy. (c) Gibbs free energy change ($G°$) at 298 K, where only vibration movements are taken into the estimation of the thermal energy and entropy. (d) Gibbs free energy change ($G°$) at 298 K in the gas-phase reaction, where translation, rotation, and vibration movements are taken into the estimation of the thermal energy and entropy.

the gas phase, because two molecules combine with each other to afford this transition state. Because this reaction is carried out in such a solvent as THF, the free energy change estimated in the gas phase is much larger than that of the real reaction.[35] We also evaluated the $\Delta G°‡$ value by considering only vibration movements where translation and rotation movements were omitted in the estimation. Thus, the estimated $\Delta G°‡$ value is −1.7 kcal/mol. It is likely that this value is too small,[47a] because this value is estimated under the assumption that the translation and rotation movements are completely suppressed in the solution. The true value is intermediate between these two values.[47b] From the intermediate **2**, the ethylene-assisted C−Si reductive elimination and the metathesis with SiH_4 take place to afford $CH_3CH_2SiH_3$ with concomitant formation of Cp_2Zr-(C_2H_4), **5**, and $Cp_2Zr(H)(SiH_3)$, **1**, respectively. The E_a and ΔE values of the ethylene-assisted reductive elimination are 26.5 (28.9) and −4.9 (−5.0) kcal/mol, respectively, and those of the metathesis are 28.3 (31.5) and −5.2 (−4.6) kcal/mol, respectively. The activation free energy ($\Delta G°‡$) and the free energy change ($\Delta G°$) of the ethylene-assisted C−Si reductive elimination are 30.4 (43.7) and 0.8 (−2.0) kcal/mol, respectively, where values without parentheses are estimated by considering only vibration movements and those in parentheses are free energy changes in the gas phase hereafter. The $\Delta G°‡$ and $\Delta G°$ values of the metathesis are 30.1 (43.9) and −2.4 (−4.8) kcal/mol, respectively. The considerably large $\Delta G°‡$ values in the gas phase are reasonably interpreted in terms that either ethylene or SiH_4 combines with $Cp_2Zr(C_2H_5)(SiH_3)$ to afford the transi-

tion state. In solution, such a big increase in the $\Delta G°‡$ value does not occur because translation and rotation movements are highly suppressed in solution. These results indicate that both the ethylene-assisted Si−C reductive elimination and the metathesis with silane occur with much difficulty in the gas phase but take place with a moderate activation energy in solution.

Starting from **5**, the coupling reaction with SiH_4 takes place to afford either $Cp_2Zr(CH_2CH_3)(SiH_3)$, **2**, or $Cp_2Zr(H)(CH_2CH_2SiH_3)$, **4**. The E_a and ΔE values of the coupling reaction leading to **2** are 0.3 (0.7) and −24.9 (−21.3) kcal/mol, respectively, as shown in Figure 9, and those of the coupling reaction leading to **4** are 5.0 (5.4) and −17.8 (−16.5) kcal/mol, respectively, as shown in Figure 10. The $\Delta G°‡$ and $\Delta G°$ values of the former coupling reaction are 2.0 (1.0) and −25.1 (−11.4) kcal/mol, respectively, and those of the latter reaction are 6.6 (6.6) and −20.7 (−7.1) kcal/mol, respectively. The reason for the much less negative $\Delta G°$ value of the gas-phase reaction is easily understood in terms that the product is formed from two molecules, $Cp_2Zr(C_2H_4)$ and SiH_4. However, the $\Delta G°‡$ value is similar to the E_a value, because the free energy difference between the precursor complex **6B** and $TS_{6B−4A}$ is taken as the $\Delta G°‡$ value (note that SiH_4 combines with $Cp_2Zr(C_2H_4)$ to afford **6B** in which entropy considerably decreases already). The intermediate **2** undergoes either the ethylene-assisted Si−C reductive elimination or the metathesis with SiH_4, as discussed above. From the intermediate **4**, the ethylene-assisted C−H reductive elimination takes place to afford $CH_3CH_2SiH_3$ with concomitant formation of $Cp_2Zr(C_2H_4)$, **5**, where the E_a and ΔE values are 5.0 (7.5) and −10.6 (−7.1) kcal/mol, respectively, as shown in Figure 10. The $\Delta G°‡$ and $\Delta G°$ values of this reductive elimination are 6.5 (19.9) and −2.8 (−5.4) kcal/mol, respectively. The $\Delta G°‡$ value in the gas phase is considerably large, because ethylene combines with $Cp_2Zr(H)(CH_2CH_2SiH_3)$ to afford the transition state in this ethylene-assisted C−H reductive elimination. On the other hand, the $\Delta G°‡$ value becomes moderately large when translation and rotation movements are not taken into consideration. Also, **4** undergoes the metathesis with SiH_4 to afford $CH_3CH_2SiH_3$ with concomitant

(47) (a) This negative activation free energy seems strange, because the transition state, $TS_{1−2A}$, is formed by two molecules. This result comes from the assumption that translation and rotation movements are completely suppressed in the solution. When only vibration movements are considered in estimation of entropy, it is not unlikely that the entropy increases upon going from $1 + C_2H_4$ to $TS_{1−2A}$, because this $TS_{1−2A}$ involves a very weak interaction between C_2H_4 and the Zr center and as a result a very small vibration frequency between them. (b) The translation and rotation movements are not completely suppressed but not completely free in the real solvent system. Thus, the true $\Delta G°‡$ value is intermediate between these two values, −1.7 and 11.6 kcal/mol, where the latter value was estimated under the assumption that translation and rotation movements are completely free.
(48) Fraga, S.; Saxena, K. M. S.; Karwowski, J. *Handbook of Atomic Data*; Elsevier Science Publ.: Amsterdam, 1976.
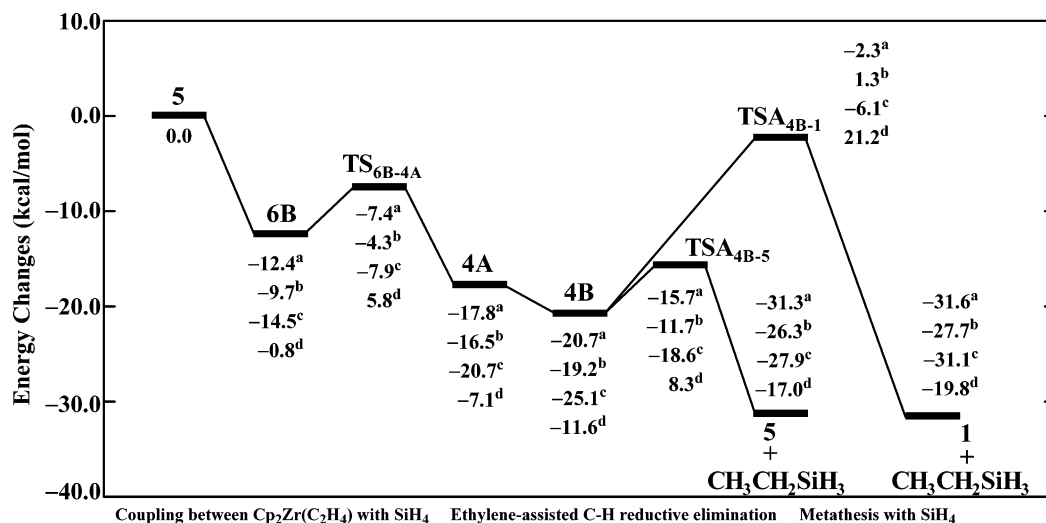
Figure 10. Energy changes in the catalytic cycle including the coupling reaction of Cp$_2$Zr(C$_2$H$_4$) with SiH$_4$, to afford Cp$_2$Zr(H)(C$_2$H$_4$SiH$_3$), followed by either the ethylene-assisted C−H reductive elimination or the metathesis with SiH$_4$ (kcal/mol unit). (a) Total energy changes without zero-point energy. (b) Total energy changes with correction of the zero-point energy. (c) Gibbs free energy change ($G°$) at 298 K, where only vibration movements are taken into the estimation of the thermal energy and entropy. (d) Gibbs free energy change ($G°$) at 298 K in the gas-phase reaction, where translation, rotation, and vibration movements are taken into the estimation of the thermal energy and entropy.
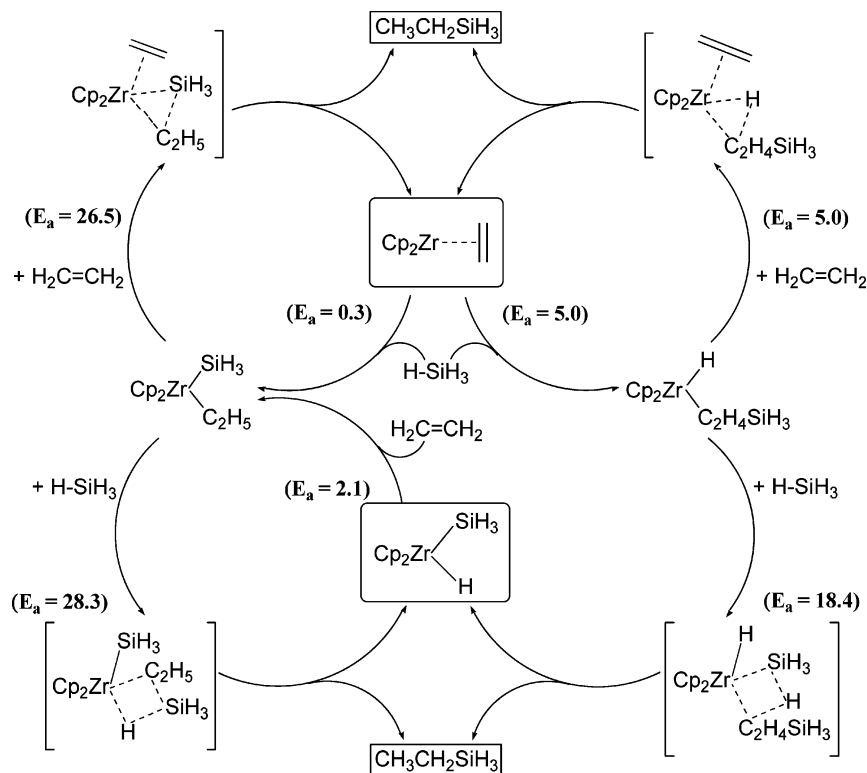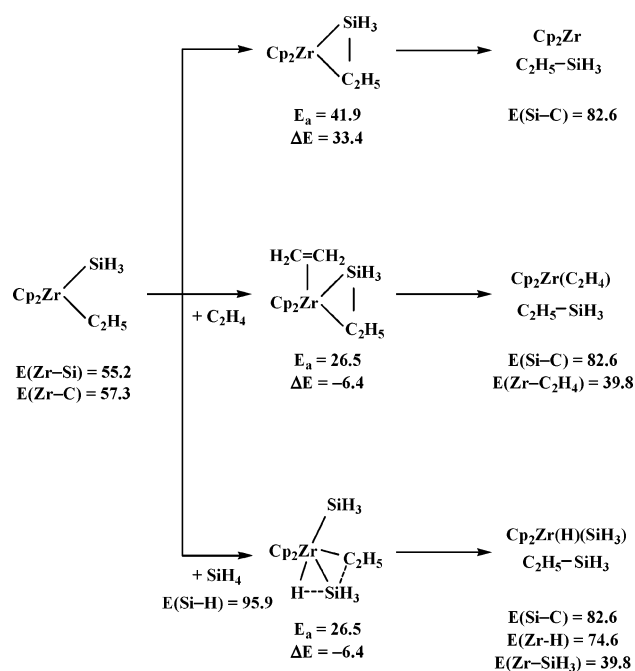

Figure 11. Theoretically proposed catalytic cycle of the Cp$_2$Zr-catalyzed hydrosilylation of alkene. Values in parentheses are the activation barrier and the energy of reaction (kcal/mol) catalyzed with the DFT/BS-II method.

formation of Cp$_2$Zr(H)(SiH$_3$), **1**, where the E_a and ΔE values are 18.4 (20.5) and −10.9 (−8.5) kcal/mol, respectively. The $\Delta G°^{\ddagger}$ and $\Delta G°$ values of this metathesis are 19.0 (32.8) and −6.0 (−8.2) kcal/mol, respectively. The considerably large $\Delta G°^{\ddagger}$ value in the gas phase is easily interpreted in terms that the transition state is formed from two molecules, Cp$_2$Zr(SiH$_3$)-(C$_2$H$_5$) and SiH$_4$, like the transition state of the ethylene-assisted C−H reductive elimination. However, the $\Delta G°^{\ddagger}$ value is moderately large when it is evaluated without translation and rotation movements. These $\Delta G°^{\ddagger}$ values suggest that both the ethylene-assisted C−H reductive elimination and the metathesis

occur with difficulty in the gas phase but they easily take place in solution. Finally, four catalytic cycles are compared in Figure 11, in which only the modified Chalk−Harrod mechanism is not involved because the ethylene insertion into the Zr−SiH$_3$ bond is very difficult. From Figures 8−11, it is clearly concluded that the most favorable catalytic cycle is the coupling reaction between Cp$_2$Zr(C$_2$H$_4$) and SiH$_4$ followed by the ethylene-assisted C−H reductive elimination.

However, we cannot neglect the possibility that Cp$_2$Zr-catalyzed hyrosilylation of ethylene proceeds through the ethylene insertion into the Zr−H bond followed by the meta-

Scheme 8 [a]

Cp₂Zr(SiH₃)(C₂H₅) E(Zr−Si) = 55.2, E(Zr−C) = 57.3

Top path: Cp₂Zr⟨SiH₃ | C₂H₅⟩, $E_a = 41.9$, $\Delta E = 33.4$ → Cp₂Zr, C₂H₅−SiH₃, E(Si−C) = 82.6

Middle path: + C₂H₄ → Cp₂Zr⟨H₂C=CH₂, SiH₃ | C₂H₅⟩, $E_a = 26.5$, $\Delta E = -6.4$ → Cp₂Zr(C₂H₄), C₂H₅−SiH₃, E(Si−C) = 82.6, E(Zr−C₂H₄) = 39.8

Bottom path: + SiH₄, E(Si−H) = 95.9 → Cp₂Zr⟨SiH₃ / C₂H₅ / H⋯SiH₃⟩, $E_a = 26.5$, $\Delta E = -6.4$ → Cp₂Zr(H)(SiH₃), C₂H₅−SiH₃, E(Si−C) = 82.6, E(Zr−H) = 74.6, E(Zr−SiH₃) = 39.8

[a] Values (in kcal/mol) are calculated with the DFT/BS-II method.

Scheme 9 [a]

Cp₂Zr(H)(C₂H₄SiH₃) E(Zr−H) = 80.7, E(Zr−C) = 57.3

Top path: Cp₂Zr⟨H | C₂H₄SiH₃⟩, $E_a = 41.9$, $\Delta E = 33.4$ → Cp₂Zr, C₂H₅−SiH₃, E(C−H) = 106.1

Middle path: + C₂H₄ → Cp₂Zr⟨H₂C=CH₂, H | C₂H₄SiH₃⟩, $E_a = 20.9$, $\Delta E = -13.5$ → Cp₂Zr(C₂H₄), C₂H₅−SiH₃, E(C−H) = 106.1, E(Zr−C₂H₄) = 39.8

Bottom path: + C₂H₄ → Cp₂Zr⟨H / C₂H₄SiH₃ / H₃Si / H⟩, $E_a = 18.4$, $\Delta E = -13.8$ → Cp₂Zr(H)(SiH₃), C₂H₅−SiH₃, E(C−H) = 106.1, E(Zr−H) = 74.6, E(Zr−SiH₃) = 56.2

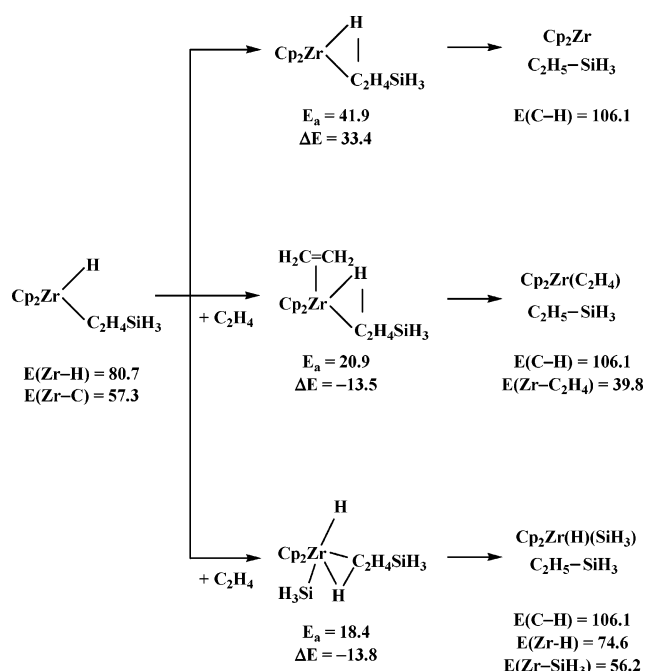[a] Values (in kcal/mol) are calculated with the DFT/BS-II method.

thesis with SiH₄, when the concentration of SiH₄ is much larger than that of ethylene. Under such conditions, **1** is formed to a much greater extent than **5**. Complex **1** easily undergoes the ethylene insertion into the Zr−H bond to afford **2**, from which the metathesis with SiH₄ takes place to afford CH₃CH₂SiH₃ with concomitant formation of **1**. Note that the ethylene-assisted Si−C reductive elimination less easily occurs than the metathesis with SiH₄ under such conditions. Corey et al.[16] and Waymouth et al.[17] experimentally proposed the metathesis of Cp₂Zr(H)(CH₂CH₂R) with hydrosilane and that of Cp₂Zr(alkyl)₂ with hydrosilane, respectively.

It should be noted that the present theoretical calculations support the experimental proposal of the coupling reaction between Cp₂Zr(alkene) and silane.[16,17] Also, new findings are presented here, as follows: The direct C−H and Si−C reductive eliminations are very difficult, but both the ethylene-assisted reductive elimination and the metatheses of Cp₂Zr(H)(CH₂CH₂SiH₃) and Cp₂Zr(CH₂CH₃)(SiH₃) with SiH₄ can occur much more easily than the direct Si−C and C−H reductive eliminations.

Reasons that Cp₂Zr(H)(CH₂CH₂SiH₃) and Cp₂Zr(CH₂CH₃)(SiH₃) Undergo Easily Ethylene-Assisted Si−C and C−H Reductive Eliminations and Metathesis with SiH₄. The reason that ethylene-assisted Si−C and C−H reductive eliminations easily take place is reasonably understood in terms of bond energies. In the direct Si−C reductive elimination, the Zr−SiH₃ and Zr−C₂H₅ bonds are broken and the Si−C bond is formed, as shown in Scheme 8. In the ethylene-assisted Si−C reductive elimination, the coordinate bond of ethylene with the Zr center is formed, in addition to the formation of the Si−C bond. The coordinate bond of ethylene is calculated to be 39.8 kcal/mol, which considerably contributes to the stabilization of the product. In the transition state, ethylene is approaching the Zr center, and the coordinate bond of ethylene with the Zr center is formed to some extent. This bonding interaction considerably contributes to the stabilization of the transition state. Essentially

the same feature is observed in the ethylene-assisted C−H reductive elimination, as shown in Scheme 9; in this case, not only C−H bond formation but also the coordinate bond of ethylene with the Zr center contributes to the stabilization of the transition states and the product, too.

Bond energies related to the metathesis are also shown in Scheme 8. In the metathesis of Cp₂Zr(CH₂CH₃)(SiH₃) with SiH₄, the Si−H bond is broken in addition to the Zr−C₂H₅ bond, while the Zr−H bond is formed in the product-side and the Zr−SiH₃ bond is still kept in the product. Thus, the product-side is very much stabilized. The same situation is observed in the metathesis of Cp₂Zr(H)(CH₂CH₂SiH₃) with SiH₄, as shown in Scheme 9.

Finally, we wish to explain the reason that the direct Si−C and C−H reductive eliminations are very difficult in the Cp₂-Zr-catalyzed hydrosilylation of alkene. As is well known, the d orbital energy becomes lower upon going to the right-hand side from the left-hand side in the periodic table, as previously calculated.[47] This means that the Zr(II) center has a d orbital at higher energy than Pt(PH₃)₂; for instance, the d_π orbital (HOMO) of Cp₂Zr is calculated to be −2.92 eV, and that of Pt(PH₃)₂ is at −4.46 eV with the DFT(B3LYP)/BS-II method, where their structures are taken to be the same as those of Cp₂Zr(C₂H₂) and Pt(PH₃)₂(C₂H₂), as typical geometry. As a result, the direct reductive eliminations of Cp₂Zr(H)(CH₂CH₂SiH₃) and Cp₂Zr-(CH₂CH₃)(SiH₃) are very difficult. We believe that this is a general trend and that both metathesis and ethylene-assisted reductive elimination play important roles in the early transition-metal complexes.

Conclusions

A new reaction mechanism of the transition-metal-catalyzed hydrosilylation of ethylene is theoretically proposed here, which involves a new type of Si−H σ-bond activation and a product release process via ethylene-assisted C−H reductive elimination.

Because the two species, Cp₂Zr(C₂H₄) and Cp₂Zr(H)(SiH₃), are similar in stability, we investigated reaction courses starting

from these two species. The ethylene insertion into the Zr—SiH$_3$ bond of Cp$_2$Zr(H)(SiH$_3$) needs a very large activation barrier (E_a = 41.8 kcal/mol), where the activation barrier calculated with the DFT(B3LYP) method is in parentheses. Thus, the Cp$_2$Zr-catalyzed hydrosilylation of alkene does not take place through the modified Chalk—Harrod mechanism. On the other hand, ethylene is easily inserted into the Zr—H bond with a very small activation barrier (E_a = 2.1 kcal/mol), to afford Cp$_2$Zr(SiH$_3$)(CH$_2$CH$_3$). Also, Cp$_2$Zr(C$_2$H$_4$) reacts with SiH$_4$ to afford Cp$_2$Zr(H)(CH$_2$CH$_2$SiH$_3$) and Cp$_2$Zr(CH$_2$CH$_3$)(SiH$_3$) with very small activation barriers of 5.0 and 0.2 kcal/mol, respectively. In general, the final step is either direct C—H or direct Si—C reductive elimination in the modified Chalk—Harrod or Chalk—Harrod mechanism, respectively. However, these direct C—H and Si—C reductive eliminations need a very large activation barrier, and moreover they are significantly endothermic. Thus, these direct reductive eliminations cannot participate in the catalytic cycle. However, the ethylene-assisted C—H and Si—C reductive eliminations easily occur with moderate activation barriers, 5.0 and 26.5 kcal/mol, respectively, and considerably large exothermicity, −13.5 and −6.4 kcal/mol, respectively. The other possible process in the product release step is metathesis of Cp$_2$Zr(H)(CH$_2$CH$_2$SiH$_3$) and Cp$_2$-Zr(CH$_2$CH$_3$)(SiH$_3$) with SiH$_4$. These metatheses take place with moderate activation barriers, 18.4 and 28.3 kcal/mol, respectively. Thus, there are three reaction courses leading to Cp$_2$Zr-(H)(CH$_2$CH$_2$SiH$_3$), **4**, and Cp$_2$Zr(CH$_2$CH$_3$)(SiH$_3$), **2**, and four reaction courses for the product release step from **2** and **4**. These results are summarized and schematically shown in Figure 11. Apparently, the most favorable catalytic cycle is the coupling reaction between Cp$_2$Zr(C$_2$H$_4$) and SiH$_4$ followed by the ethylene-assisted C—H reductive elimination.

On the other hand, when SiH$_4$ exists in excess in the solution but ethylene does not sufficiently exist in the solution, Cp$_2$Zr-(H)(SiR$_3$), **1**, is formed to a much greater extent than Cp$_2$Zr-(C$_2$H$_4$), **5**, because **1** and **5** are in thermal equilibrium with each others. Under such conditions, **1** plays the role of an active species and the Cp$_2$Zr-catalyzed hydrosilylation of ethylene takes place through the ethylene insertion into the Zr—H bond followed by the metathesis of Cp$_2$Zr(SiR$_3$)(C$_2$H$_5$) with SiH$_4$, to afford the product with concomitant formation of Cp$_2$Zr(H)-(SiH$_3$).

It is of considerable interest to clarify the reason that Cp$_2$-Zr-catalyzed hydrosilylation takes place through the coupling reaction, unlike the platinum- and rhodium-catalyzed hydrosilylation of alkene. One of the characteristic features of Cp$_2$Zr is that the 4d orbital of the Zr center is at a high energy; in other words, Cp$_2$Zr(C$_2$H$_4$) involves a very strong d$_\pi$-π* back-donation interaction between the Zr center and ethylene, due to the strong Lewis basicity. The coupling reaction between Cp$_2$-Zr(C$_2$H$_4$) and SiH$_4$ proceeds through the bonding overlap between the Si—H σ*-orbital and d$_\pi$-π* back-donation orbital. Because of the strong Lewis basicity of Cp$_2$Zr, the direct Si—C and C—H reductive elimination cannot occur, but both ethylene-assisted C—H and Si—C reductive eliminations, as well as metathesis of Cp$_2$Zr(H)(CH$_2$CH$_2$SiH$_3$) and Cp$_2$Zr(SiH$_3$)(CH$_2$-CH$_3$) with SiH$_4$, participate in the product release step.

In conclusion, this reaction mechanism including the new type of Si—H σ-bond activation arises from the fact that Cp$_2$Zr has an occupied d orbital at high energy; in other words, the occupied d orbital of the Cp$_2$Zr catalyst at high energy leads to significant differences in the reaction mechanism of the Cp$_2$Zr catalyst and the mechanisms of others such as Pt(0) and Rh(I) catalysts.

Supporting Information Available: Figure of transition state structures with imaginary frequency and the important movements of each nuclei in the imaginary frequency. Figure of energy changes along the catalytic cycle including ethylene insertion into the Zr—H bond followed by the direct Si—C reductive elimination and that including ethylene insertion into the Zr—SiH$_3$ bond followed by the direct C—H reductive elimination. Cartesian coordinates of important species including transition states (PDF). This material is available free of charge via the Internet at http://pubs.acs.org.

JA0304345